Journal of Vertebrate Paleontology

ISSN: 0272-4634 (Print) 1937-2809 (Online) Journal homepage: www.tandfonline.com/journals/ujvp20

Novel record of placodont remains including a *Henodus* cranium from the Upper Triassic Silves Group of the Algarve, southern Portugal

Maciej Ruciński, Hugo Campos, Octávio Mateus & Ingmar Werneburg

To cite this article: Maciej Ruciński, Hugo Campos, Octávio Mateus & Ingmar Werneburg (2024) Novel record of placodont remains including a *Henodus* cranium from the Upper Triassic Silves Group of the Algarve, southern Portugal, Journal of Vertebrate Paleontology, 44:5, e2460445, DOI: 10.1080/02724634.2025.2460445

To link to this article: https://doi.org/10.1080/02724634.2025.2460445

Journal of Vertebrate Paleontology e2460445 (23 pages)
Published with license by the Society of Vertebrate Paleontology.
DOI: 10.1080/02724634.2025.2460445

ARTICLE

NOVEL RECORD OF PLACODONT REMAINS INCLUDING A *HENODUS* CRANIUM FROM THE UPPER TRIASSIC SILVES GROUP OF THE ALGARVE, SOUTHERN PORTUGAL

MACIEJ RUCIŃSKI, [1,2*] HUGO CAMPOS,[3,4] OCTÁVIO MATEUS, [2] and INGMAR WERNEBURG [5,6]
[1]Natural History Museum, University of Oslo, P.O. Box 1172 Blindern, NO-0318 Oslo, Norway, maciej.rucinski@nhm.uio.no;
[2]GeoBioTec and Department of Earth Sciences, NOVA School of Science and Technology, Universidade Nova de Lisboa, Portugal, omateus@fct.unl.pt;
[3]Loulé Municipal Museum, Portugal, hugo.campos@cm-loule.pt;
[4]Algarvensis aspiring UNESCO Global Geopark, Portugal;
[5]Fachbereich Geowissenschaften der Universität Tübingen, Paläontologische Sammlung, Hölderlinstraße 12, 72074, Tübingen, Germany;
[6]Senckenberg Center for Human Evolution and Palaeoenvironment an der Universität Tübingen, Sigwartstraße 10, 72076, Tübingen, Germany, ingmar.werneburg@senckenberg.de

ABSTRACT—Recent fieldwork in the Upper Triassic deposits of the Silves Group in the Algarve, southern Portugal revealed novel cyamodontid placodont material. The collection includes a partial skull and numerous isolated armor plates from four localities in Silves and Loulé municipalities. The skull shows a strong affinity to henodontid placodonts, especially to *Henodus chelyops* from Tübingen-Lustnau in Germany. It shares features such as a rectangular outline of the cranium, occurrence of a broad spatulate rostrum, and toothless maxillae with curved longitudinally extending grooves. The only unambiguous difference observed pertains to the more robust and convex snout shape of the new specimen. Based on these multiple similarities, the specimen is identified as *Henodus* sp., but poor preservation prevents species-level identification. The new specimen from Portugal represents the second record of *Henodus* and illustrates a wider geographic distribution of that genus, extending beyond the Germanic Basin and reaching coastal areas near the westernmost branch of the Neotethys. The age of the deposits where the cranium was found is not well-established but refers to a time interval within the upper Carnian–Rhaetian, suggesting the specimen may be younger than other henodontid records. The novel *Henodus* material found in the continental, but likely the near-coastal depositional setting, concurs with the known records of brackish to the freshwater habitat of the other henodontid placodonts. The occurrence of abundant armor plates assigned to Cyamodontidae at multiple sites and stratigraphic horizons indicates that placodonts were common in the south Iberian margin.

SUPPLEMENTARY FILE(S)—Supplementary file(s) are available for this article for free at www.tandfonline.com/UJVP

Citation for this article: Ruciński, M., Campos, H., Mateus, O., & Werneburg, I. (2025) Novel record of placodont remains including a *Henodus* cranium from the Upper Triassic Silves Group of the Algarve, southern Portugal. *Journal of Vertebrate Paleontology*. https://doi.org/10.1080/02724634.2025.2460445

Submitted: September 12, 2024
Revisions received: January 14, 2025
Accepted: January 15, 2025
First published online: March 11, 2025

INTRODUCTION

The Triassic was an important period for vertebrate communities, which underwent a substantial change in faunal composition and ecological structure (e.g., Benton, 2014; Benton & Wu, 2022). In the aftermath of the Permian–Triassic extinction, novel taxa took over the dominance in the seas (Benton & Wu, 2022; Benton et al., 2013). Among them were several lineages of the Mesozoic marine reptiles, which as a result of the broad success in adaptation to marine environments underwent their first major radiation. Consequently, new taxa evolved including ichthyopterygians, thalattosaurs, and sauropterygians (Motani, 2009; Renesto & Dalla Vecchia, 2018; Rieppel et al., 2000; Scheyer et al., 2014). Sauropterygia Owen, 1860, constituted the monophyletic sauropsid group within the proposed clade Sauropterygomorpha Wolniewicz et al., 2023, which quickly diversified during the Triassic. The main representatives of Sauropterygia were placodontiforms, including placodonts, and eosauropterygians. The latter encompassed nothosauroids, pachypleurosaurs, and pistosauroids (Benton, 2014; Motani, 2009; Rieppel et al., 2000).

Placodonts were turtle-like (including armored and carapace-lacking taxa), medium-sized, usually around 1–2 m long reptiles with uncontested fossil record bracketing the early Middle to

*Corresponding author.

Color versions of one or more of the figures in the article can be found online at www.tandfonline.com/ujvp.

latest Triassic (Neenan et al., 2013, 2015; Norden et al., 2015; Pinna, 1990; Pinna & Nosotti, 1989; Rieppel et al., 2000). Those marine reptiles inhabited shallow seas of the north-western and north-eastern Tethys, which correspond to the occurrences in the modern areas of Europe (i.e., Buffetaut & Novak, 2008; de Miguel Chaves et al., 2015, 2020a; Gere et al., 2020; Klein & Scheyer, 2013; Neenan & Scheyer, 2014; Norden et al., 2015; Pinna & Mazin, 1993; Pinna & Nosotti, 1989; Rieppel, 2001, 2002b; Rieppel et al., 2000), Middle East (Haas, 1967, 1969; Rieppel, 2002b), and East Asia (Jiang et al., 2008; Li & Rieppel, 2002; Wang et al., 2019a, 2019b, 2020; Zhao et al., 2008). During the Anisian stage, placodonts diversified into the placodontids–a carapace-lacking group traditionally referred to as Placodontoidea von Nopcsa, 1923, but often resolved as paraphyletic, and the monophyletic Cyamodontoidea von Nopcsa, 1923 (Wang et al., 2019a, 2020, 2022).

In contrast to the representatives of placodontoids, the cyamodontoid placodonts possessed a well-developed carapace composed of dermal armor plates (Rieppel, 2002b; Scheyer, 2007; Wang et al., 2020; Westphal, 1976), while a few representatives also developed a plastron (Rieppel, 2002b; Westphal, 1976). Their shells were overall similar in shape to those of turtles, or bipartite like in *Cyamodus* (Rieppel, 2002b; Scheyer, 2010). Unlike in turtles, the placodont carapaces were not fused with the ribs and vertebrae, instead being sustained by the expanded transverse processes of vertebrae (Lyson et al., 2016; Rieppel, 2002b; Scheyer, 2010; Schoch & Sues, 2020). Most placodont representatives were characterized by robust wide skulls with large temporal fenestrae and massive flattened oval tooth plates, constituting adaptations to a durophagous diet (Maisch, 2020; Pommery et al., 2021; Rieppel, 2002a; Scheyer et al., 2011). Those features combined with a pachyostotic skeleton suggest that those animals were bottom dwellers consuming hard-shelled invertebrate prey (Pommery et al., 2021; Rieppel, 2002a; Scheyer et al., 2011).

One of the most morphologically distinct yet extremely rare and poorly understood groups among Cyamodontoidea are the henodontid placodonts. Henodontidae von Huene, 1936, is represented by *Henodus chelyops* von Huene, 1936, and *Parahenodus atancensis* de Miguel Chaves et al., 2018a. *H. chelyops is* exclusively known from the lower Carnian deposits of Goldersbach, located near Tübingen-Lustnau in southwestern Germany, where seven skulls and eight almost complete skeletons were found (Fischer, 1959; Pommery et al., 2021; von Huene, 1936, 1938, 1958; Werneburg, 2021; Werneburg & Böhme, 2018). The second henodontid species, *P. atancensis*, is known solely from the posterior part of the cranium (de Miguel Chaves et al., 2018a, 2020c) recovered in the early Carnian locality El Atance in Spain (García-Ávila et al., 2021). *Parahenodus* has been recovered from restricted marine lagoonal deposits (García-Ávila et al., 2021), while *Henodus* remains are derived from brackish to freshwater settings (Aigner & Bachmann, 1989; Pommery et al., 2021; Reif & Stein, 1999; Reiff, 1937), differentiating both taxa from remaining representatives of Placodontia recorded in shallow marine facies (Rieppel, 2002b; Rieppel et al., 2000; Scheyer et al., 2011).

Henodus chelyops skeleton can be distinguished based on the massive fusiform carapace composed of equilateral to elongated hexagonal dermal armor plates and gracile short limbs (Rieppel, 2002b; von Huene, 1936, 1938; Werneburg, 2021; Westphal, 1976). Exhibiting multiple autapomorphies, the broad but flat rectangular-shaped skull is characterized by a reduced dentition to the pair of palatine teeth, occurrence of maxillary grooves, a cutting edge with neomorphic denticles on the premaxillae, and reduced to closed temporal fenestrae (Pommery et al., 2021; Reif & Stein, 1999; Rieppel, 2001, 2002a; Rieppel et al., 2000; von Huene, 1936). The cranial fragment of *P. atancensis* also exhibits reduced dentition and temporal fenestrae, but at the same time preserves the plesiomorphic cranial shape characteristic for cyamodontoid placodonts consisting of the anteriorly narrowing rostrum (de Miguel Chaves et al., 2018a, 2020c). The distinctly different skull morphology from remaining representatives of Cyamodontidae suggests henodontid placodonts occupied different 'niches,' likely either as filter-feeders, herbivores, or generalists (Chun et al., 2016; Gere et al., 2024; Pommery et al., 2021; Reif & Stein, 1999; Rieppel, 2002a).

The substantially scarce material of Henodontidae and its remarkably distinctive morphological characters make the interpretation of the evolutionary history, paleobiology, and paleobiogeography of that clade especially challenging. Thus, any new record of henodontid placodonts has the potential to largely improve the knowledge about these enigmatic animals. In the present paper, we present such material from the Algarve.

The vertebrates of the Triassic of the Algarve have been known since at least 1895 from São Bartolomeu de Messines (Silves Municipality) but were not published as such. In 1897, Henri-Émile Sauvage published one of the first major studies on fossil vertebrates in Portugal, based on the specimens supplied by Paul Choffat from the Portuguese Geological Surveys (nowadays LNEG). Although he did not report any Triassic vertebrates, the letter from Paul Choffat to Sauvage dated July 30, 1895 (LNEG archive unpublished archived letter, reference PT LNEGCG03.01.49), lists all fossil vertebrates stratigraphically ordered. This six-page list includes the existence of vertebrates from the Triassic of São Bartolomeu de Messines but lacks any further taxonomic identification. Choffat later mentioned that he never visited the locality himself (1904:84).

In the 1970s, Christian Palain briefly noted in his doctoral thesis, that stegocephalian remains (Palain, 1976:117, pL VIII, fig. 4) were recovered west to São Bartolomeu de Messines. This material has remained unpublished in the Geological Museum in Lisbon ever since and is here addressed (see below). The Triassic vertebrate site of São Bartolomeu de Messines was for the first time studied in more detail by Russell and Russell (1977), who also recovered more bone fragments. It is unclear whether the fossil site described by Russell and Russell (1977) is the same one that Choffat reported.

More to the east, in Loulé Municipality, further prospecting was conducted in 1979 and 1980 by Thomas Schröter as part of his thesis. The collected fossils of this thesis represent temnospondyl material and were described by Witzmann and Gassner (2008). During the first large-scale excavations in the Upper Triassic of the Algarve conducted in the 2010s at the site near Rocha da Pena, novel vertebrate material has been discovered. That included a mandible and isolated teeth of a phytosaur (Mateus et al., 2014) and numerous temnospondyl remains derived from the bonebed, assigned to a new species, *Metoposaurus algarvensis* (Brusatte et al., 2015).

Continued fieldwork, focusing on carbonate beds at the Penina and Vale de Álamo sites as well as localities in São Bartolomeu de Messines and Vale Vinagre, revealed the occurrence of isolated cyamodontoid dermal armor plates (Campos & Mateus, 2018; Ruciński, 2020). These included the elongated hexagonal types (Campos & Mateus, 2018), resembling the armor plates located in the central part of the *H. chelyops* carapace (Campos & Mateus, 2018; von Huene, 1936, 1938; Westphal, 1976). In 2018, a fragment of a henodontid cranium was found at the Vale de Álamo site by Jorge Graça and donated to Museu Municipal de Loulé. The main aim of the present study was to provide an osteological description and taxonomic interpretation of this cranial fragment, which reveals affinity to henodontid placodonts. Moreover, among the postcranial elements recovered, we present the material which can be at this point unambiguously attributed, as armor dermal plates, to cyamodontoid placodonts. Lastly, we discuss the implications of the novel material on paleobiogeography, temporal range, and paleoecology of henodontid placodonts, as well as the integration of placodont material into the local paleontological context.

GEOLOGICAL SETTING

The placodont material was found at four sites located in the Algarve region, southern Portugal, including Penina and Vale do Álamo near Rocha da Pena, São Bartolomeu de Messines, and Vale Vinagre (Fig. 1A–C). All investigated outcrops represent the Upper Triassic deposits of the Algarve Basin (Azerêdo et al., 2003; Brusatte et al., 2015; Palain, 1976, 1979; Rocha, 1976; Terrinha et al., 2006, 2019). Those deposits were originally assigned to the informal unit 'Gres de Silves' by Choffat (1887), which is now substituted by the overall stratigraphically equivalent term 'Silves Group' of the Algarve Basin (Fig. 1D) (Soares et al., 2012).

There are several stratigraphic divisions of the early Mesozoic portion of the Algarve Basin (Manuppella, 1992; Palain, 1976, 1979; Pratsch, 1958; Rocha, 1976; Teixeria, 1942), which were summarized by Azerêdo et al. (2003). Here we adopt the most recent terminology of Vilas-Boas et al. (2021, 2022, 2024), which is based on the stratigraphic divisions proposed by Manuppella (1992). Based on those interpretations, the Early Mesozoic succession of the Algarve can be divided into three main units starting with Silves Sandstones (also known as 'Gres de Silves' sensu Rocha, 1976, or unit AB1 sensu Palain, 1976, 1979) corresponding to the sandstones and conglomerates deposited in fluvial settings. The latter unit is overlaid by the Silves Marl-Carbonate Evaporitic Complex (AB2 unit sensu Palain, 1976, 1979) representing coastal mudflat with fine-grained siliciclastic, carbonate, and evaporite deposition (Azerêdo et al., 2003; Palain, 1979; Terrinha et al., 2019; Vilas Boas, 2023; Vilas-Boas et al., 2021, 2024). The upper portion of the Silves Group consists of the Volcano-Sedimentary Series built of volcaniclastic and volcanic rocks, interpreted to be related to the Central Atlantic Magmatic Province (Martins et al., 2008; Pérez-López et al., 2021; Verati et al., 2007; Youbi et al., 2003).

Based on the interpretations of Palain (1976, 1979) and Russel and Russel (1977), the São Bartolomeu de Messines (SBM) outcrop (Figs. 1D, S10–S11), composed of lutites (mudstones to very fine sandstones) and thin carbonates, might represent the locally occurring basal part of Silves Sandstone, currently termed as São Bartolomeu de Messines Claystones (unit AA sensu Palain, 1976, 1979). Thus, it may correspond to the base of Silves Group in the Algarve, recently dated as Carnian (Vilas-Boas et al., 2022). However, the absence of distinct layers that could enable correlation with other outcrops leaves the stratigraphic position of the SBM outcrop uncertain (Campos et al., 2017). Penina and Vale do Álamo sites are attributed to the upper portion of the Silves Marl-Carbonate Evaporitic Complex (Figs. 1D, S12–S13). This unit has been referred to be Carnian–Norian age (Brusatte et al., 2015), with recent palynological data implying upper Carnian to Rhaetian and possibly

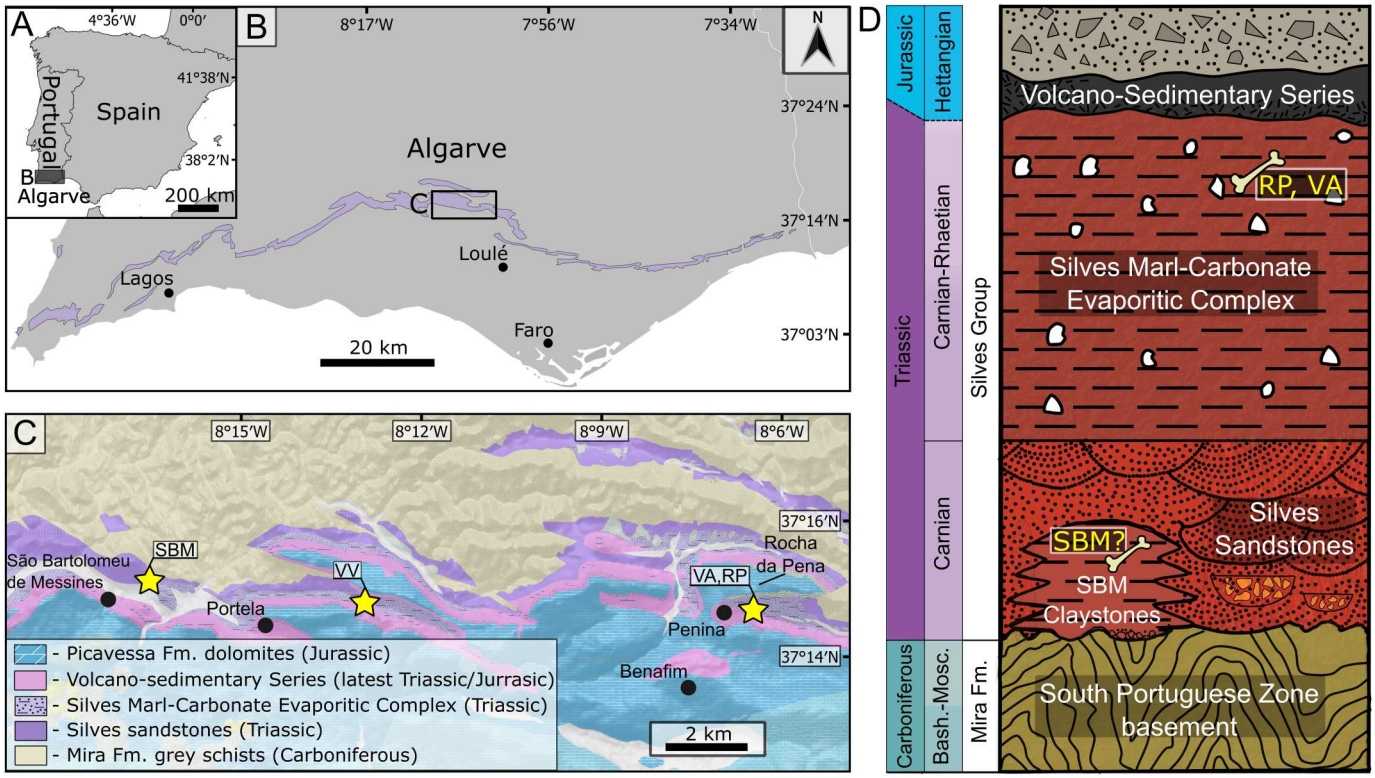

FIGURE 1. Geographic and stratigraphic contexts of the Late Triassic material investigated from the Algarve region in southern Portugal. **A**, map of the Iberian Peninsula with indicated location of the Algarve region. **B**, map of the Algarve with Triassic exposures (modified from LNEG Geological Map of the Algarve Region, scale 1:100,000). **C**, geological map (modified from LNEG Geological Map of the Algarve Region, scale 1:100,000, 1992) showing localities where cyamodontoid placodont material has been found (indicated by stars). **D**, synthetic stratigraphy of the Silves Group in the Algarve Basin (after Manuppella, 1992) with English terminology and chronostratigraphic ascriptions of Vilas-Boas et al. (2024). SBM site is here tentatively attributed to 'São Bartolomeu de Messines Claystones' (the locally occurring basal unit of Silves Sandstone, which is (likely lower) Carnian in age; Vilas-Boas et al., 2021) following historical ascription (AA unit sensu Palain, 1976, 1979). However, the stratigraphic placement of the SBM site remains uncertain, with the alternative possibility of assignment to the Silves Marl-Carbonate Evaporitic Complex still under consideration. VA and RP sites correspond to Silves Marl-Carbonate Evaporitic Complex, estimated to be upper Carnian to Rhaetian-Hettangian in age (AB2 unit sensu Palain, 1976, 1979). The fossiliferous beds from the sites investigated are at this point attributed to the upper portion of the latter unit; however, the occurrence of a local hiatus in the section is also possible. VV site lacks precise stratigraphic assignation but refers to the Triassic deposits of the Silves Group. **Abbreviations**: **RP**, Rocha da Pena; **SBM**, São Bartolomeu de Messines; **VA**, Vale do Álamo; **VV**, Vale Vinagre.

even up to Hettangian age range (Vilas-Boas et al., 2024). However, the exact age of Penina and Vale do Álamo deposits remains uncertain due to the lack of biostratigraphically reliable and informative taxa, and a problematic regional correlation with already dated sites. The so-far recorded faunal assemblage appears to be most concordant with the Carnian–Norian age; nonetheless, younger age cannot be excluded at this point. Stratigraphy of the Vale Vinagre site has not yet been established, thus its precise age remains unsure, although lithological characteristics resembling deposits of the Silves Marl-Carbonate Evaporitic Complex point to the Upper Triassic age.

The herein-described specimens were found at multiple horizons of gray to light green calcareous siltstones/claystones or palustrine carbonate beds (see Figures and descriptions in Supplementary File 1). Those layers are usually thin (10–20 cm) and constitute the part of the rock sequences mostly composed of variegated, but prevalently red to brown mudstones interbedded with carbonates and evaporites (Figs. S1–2, S8–S11). The deposition of those layers took place under a semi-arid climate in the floodplain to palustrine environments, likely in the coastal area in proximity to the western-most branch of the Neotethys (Azerêdo et al., 2003; Lopes, 2014; Palain, 1976; Ruciński, 2020; Vilas-Boas et al., 2024).

MATERIAL AND METHODS

Fossil Specimens and Preparation

Studied samples include armor plates and fragments of bones collected during the authors' fieldwork, a revised specimen (MG specimen unnumbered) collected by and briefly mentioned by Palain (1976), and the donated specimen ML. A9182 (ML = Museu Municipal de Loulé, Portugal). Most of the gathered collection (a few dozen specimens) is represented by fragments of dermal armor plates.

The herein presented collection comprises the cranial fragment with associated armor dermal plate (ML. A9182), an example of five better preserved isolated dermal plates (FCT-UNL 628; 630; 715; 717; 719), and a block containing numerous dermal plates and bone fragments of variable state of preservation (FCT-UNL 714). Moreover, a specimen from Museu Geológico de Lisboa (MG specimen unnumbered) consisting of a small limestone block with fragments of armor plates, originally collected by Palain (1976) and identified (briefly described but not depicted) as stegocephalian indeterminate elements, is herein redescribed.

Specimens were collected from both isolated blocks and directly from fossiliferous layers. The cranial fragment ML. A9182 was found by Jorge Graça on the slope of Vale do Álamo exposure (Fig. S1) in an isolated block (Fig. S6), which he donated to Museu Municipal de Loulé in 2019. Based on sedimentological (Figs. S2, S3) and geochemical investigations (Figs. S4, S5), the stratigraphic position from which ML. A9182 is most likely derived was identified (Fig. S2). The remaining specimens are deposited at the Departamento de Ciências da Terra of Faculdade de Ciências e Tecnologia of Universidade Nova de Lisboa. The block FCT-UNL 714 (field number: Messines 10), containing the cyamodontoid specimens from the layer IC1722-2 and collected in São Bartolomeu de Messines, was extracted after covering it with a jacket of plaster and burlap. In Vale Vinagre, two dermal armor plates were found in an isolated carbonate block.

Specimen ML. A9182 and other newly obtained specimens were prepared in Dinoparque Lourinhã, Departamento de Ciências da Terra of Faculdade de Ciências e Tecnologia of Universidade Nova de Lisboa, and the laboratory at Museu da Lourinhã, using air scribes of different sizes and tungsten needle. In the case of a few specimens, 10% hydrochloric acid (HCl) was used to dissolute the carbonated parts of rock covering fossils (performed at Departamento de Ciências da Terra of Faculdade de Ciências e Tecnologia of Universidade Nova de Lisboa). The hydrochloric acid was applied by a brush on the rock to ensure a small amount of acid was delivered in the specific places. In case of appearing breakages, the 5% and 50% Paraloid B-72 diluted in acetone was used as consolidation. Big cracks occurring in fossils were filled with 50% and 70% Paraloid B-72. While preparing the block FCT-UNL 714, the cracks were filled with polyethylene glycol (Carbowax) to retain the block consistency.

Documentation and a 3D Visualization

Specimens were photographed with Canon EOS 50D. Photographs and illustrations were further processed and compiled into figures in Adobe Illustrator CS6 and Inkscape (v.1.3.2). ML. A9182 was photographed before (Fig. S6), during (Figs. S6, S7), and after the preparation (Figs. 4–6).

A 3D photogrammetry model of ML. A9182 has been obtained in Reality Capture (version 1.4). In total, 418 photos of the ML. A9182 were taken. Photos were aligned using a medium image overlap setting and a maximum 40,000 features per image. A high-detail model was processed resulting in 15 million vertices and 29.8 million polygons. The model was textured using the maximal texture count method and triangle removal threshold set at 10,000 resulting in one texture count with a resolution of 16,384 × 16,384 pixels. For easier use, the model was further simplified to two versions with 4 million and 750,000 polygons. In the case of both models, they were unwrapped, and texture was reprojected from the highest quality model resulting in one texture count of 8192 × 8192 pixels. Models were exported in ply. format. The 750,000-polygon model is available as Supplementary File 7 and the online version of this article. The 4 million polygon model can be accessed via Morphobank project 5220 at http://morphobank.org/permalink/?P5625. Renders of ML. A9182 digital version based on the original high-detail photogrammetry model are available in the Supplementary materials (Figs. S8, S9).

Phylogenetic Analyses

For phylogenetic analysis in TNT (version 1.6, January 2024), one primary and three secondary data matrices (presented in Supplementary Files) were used to test the relationships of ML. A9182. The secondary datasets include a hypothetical all-zero ancestor as an outgroup taxon, which makes them suboptimal for analyzing real-world scenarios. However, by encompassing varying degrees of taxonomic inclusiveness and incorporating both total and cranial-only character matrices, these complementary analyses enable testing the phylogenetic placement of ML. A9182 across different scenarios and facilitate comparisons with previously obtained results on placodont phylogeny.

The first analysis (Analysis 1) was performed based on the comprehensive, species-based, diapsid dataset of Wang et al. (2022), which represents an extended dataset of Neenan et al. (2015) and Wang et al. (2019a). This dataset was selected for its extensive coverage of Mesozoic diapsids, including the most up-to-date scoring of placodonts. The dataset includes *Youngina capensis* as an outgroup. In total, 181 morphological characters and 63 taxa including ML. A9182 were analyzed (Supplementary File 3).

A second analysis (Analysis 2) was performed based on the comprehensive diapsid dataset of Neenan et al. (2015) with modifications by Wang et al. (2019a). This dataset includes taxa at various taxonomic levels, encompassing species, genera, and larger suprageneric clades, with an all-zero ancestor as an outgroup taxon. The data matrix included 140 cranial and postcranial characters and 54 taxa including ML. A9182 (Supplementary File 4). The scoring of character 29 was changed for *Henodus chelyops* from (01) to (34) based on the

observation of seven skull specimens (GPIT-PV-30001–GPIT-PV-30007). This analysis was used to assess how the character set from Wang et al. (2022) and the taxonomic inclusivity of the selected taxa influenced the phylogenetic placement of ML. A9182.

A third matrix (Analysis 3) of 63 cranial characters was obtained from the cranial dataset of Neenan et al. (2015). Including data on ML. A9182 and *Parahenodus atancensis* (de Miguel Chaves et al., 2018a), a total of 18 placodont species were compared, with an all-zero ancestor as an outgroup taxon (Supplementary File 5). This dataset was chosen due to its focus on cranial characters, reducing the amount of non-scorable characters for ML. A9182. The results of this analysis were compared with a revised scoring (Analysis 4) of *H. chelyops* (Supplementary File 6, for an explanation of changes in scoring see Supplementary File 1).

The traditional search was applied with 1000 replications of Wagner trees together with the branch swapping (TBR) options with 10 trees saved for replication. All character states had the same weight and were unordered. Based on the obtained data, a consensus tree was created. CI, RI, and RC were calculated, as well as Bremer and bootstrap decay values (number of replicates: 1000) to assess the robustness of support for each node. The data matrices were edited using Mesquite Version 3.81 (Maddison & Maddison, 2011). Data matrices and phylogenetic trees are presented in the Supplementary Files. The data matrices, characters list, and additional images are also available in Morphobank project 5220 at http://morphobank.org/permalink/?P5625.

Institutional Abbreviations—FCT-UNL, Faculdade de Ciências e Tecnologia, Universidade Nova de Lisboa, Caparica, Portugal; **GPIT**, Paläontologische Sammlung der Universität Tübingen, Tübingen, Germany (acronym based on the former: Geologisch-paläontologisches Institut der Universität Tübingen); **MG**, Museu Geológico, Lisbon, Portugal; **ML**, Museu Municipal de Loulé, Loulé, Portugal.

SYSTEMATIC PALEONTOLOGY

SAUROPTERYGIA Owen, 1860
PLACODONTIFORMES Neenan, Klein, and Scheyer, 2013
PLACODONTIA Cope, 1871
CYAMODONTOIDEA indet.
(Figs. 2, 3)

Material—Isolated dermal plates or their fragments represented in this work by the five best-preserved specimens (FCT-UNL 628; 630; 715; 717; 719); isolated dermal plate in ML. A9182 block also containing the cranial fragment; block with dermal plates and unidentified bone fragments (FCT-UNL 714), uncataloged specimen from Museo Geologico in Lisbon consisting of block with fragmentary armor plates (see Table S1 for details regarding the presented material).

Locality—Rocha da Pena (Municipality of Loulé, Parish [Freguesia] of Benafim, ca. 37.2516°N, −8.1109°W); Vale do Álamo (Municipality of Loulé, Parish [Freguesia] of Salir, ca. 37.249° N, 8.107°W); Vale Vinagre Municipality of Loulé, Freguesa of Alte, ca. 37.251611°N, 8.217278°W), and São Bartolomeu de Messines IC1722 (Municipality of Silves, Freguesia of São Bartolomeu de Messines (ca. 37.254°N, 8.273°W).

Horizon and Age—Silves Group, possibly São Bartolomeu de Messines Claystones (also known as AA unit sensu Palain (1976, 1979)—basal part of Silves Sandstones, (likely early) Carnian; Upper Triassic; Silves Marl-Carbonate Evaporitic Complex (also known as AB2 unit sensu Palain (1976, 1979) or 'Pelitos com evaporitos e intercalações carbonatadas' sensu Manuppella (1992); Upper Triassic (age uncertain, within upper Carnian–Rhaetian).

CYAMODONTIDA von Nopcsa, 1923
HENODONTIDAE von Huene, 1936
HENODUS sp.
(Figs. 4–7)

Material—ML. A9182 representing a large fragment of a cranium, missing the premaxillae, right lateral, and the posterior-most portion of the skull.

Locality—Vale do Álamo near Rocha da Pena, Municipality of Loulé, Parish [Freguesia] of Salir, the Algarve, southern Portugal, approximated coordinates 37.249°N, 8.107°W.

Horizon and Age—Silves Group, upper part of Silves Marl-Carbonate Evaporitic Complex (also known as AB2 unit sensu Palain 1976, 1979) or 'Pelitos com evaporitos e intercalações carbonatadas' sensu Manuppella (1992); Upper Triassic.

DESCRIPTION AND COMPARISON

Armor Plates

Description—The cyamodontoid fossil record of the Algarve includes numerous isolated dermal armor plates, which constituted elements of the carapace (Fig. 2A–I). The largest complete specimen (FCT-UNL 715) is 4.6 cm long, 2.7 cm wide, and 0.3 cm thick (Fig. 2B). The smallest nearly complete (Fig. 2H) armor plate (FCT-UNL 717) is 3.3 cm long, 2.1 cm wide, and 0.3 cm thick (an armor plate within the block ML. A9182 represents a smaller plate but is incomplete.) The collected material is composed of armor plates of different shapes and highly varying degrees of preservation. The best-preserved armor plates can be divided into two morphotypes: (1) a hexagonal, but laterally expanded type, being approximately two times wider than long (Fig. 2A–F), and (2) a mostly hexagonal or heptagonal, equilateral type of bone plates (Fig. 2G–I).

The margins of most of the elongated hexagonal dermal plates (morphotype 1) are overall poorly preserved, exhibiting signs of breakage or cracking. Some specimens have a minute millimeter-size, laterally extending triangular protrusions (Fig. 2A), being well-developed within one of the dermal plates' margins, with the remaining edges of the bone plates exhibiting straight borders (Fig. 2A). However, in the case of worse-preserved specimens of this morphotype (represented by FCT-UNL 715), protrusions are not visible (Fig. 2B). The described protrusions refer to interdigitating sutures between the plates originally forming a carapace (de Miguel Chaves et al., 2020a; Rieppel 2002b). All bone plates of morphotype 1 are planar with either smooth surfaces or very weakly developed radial striations composed of minute ridges and grooves, with locally observed millimeter-scale pitting (Fig. 2A–E).

The equilateral hexagonal or heptagonal armor plates (morphotype 2; represented by FCT-UNL 628, FCT-UNL 717, and armor plate from ML. A9182 block), have straight or slightly undulating margins (Fig. 2G–I). In the case of the FCT-UNL 628 (Fig. 2G) the medial portion of the armor plate is slightly upraised and keeled resulting in a low-triangle shape in the transverse section. The low keel extends longitudinally throughout most of the preserved part of the medial extent of the armor plate (Fig. 2G). The dorsal surface within the central area of the armor plate is strongly perforated. Distally, the surface sculpture is dominated by radial ornamentation composed of minute irregular ridges and grooves (Fig. 2G).

A specimen from São Bartolomeu de Messines was originally identified as a rock fragment containing stegocephalian remains (Palain, 1976). This specimen is here redescribed as an

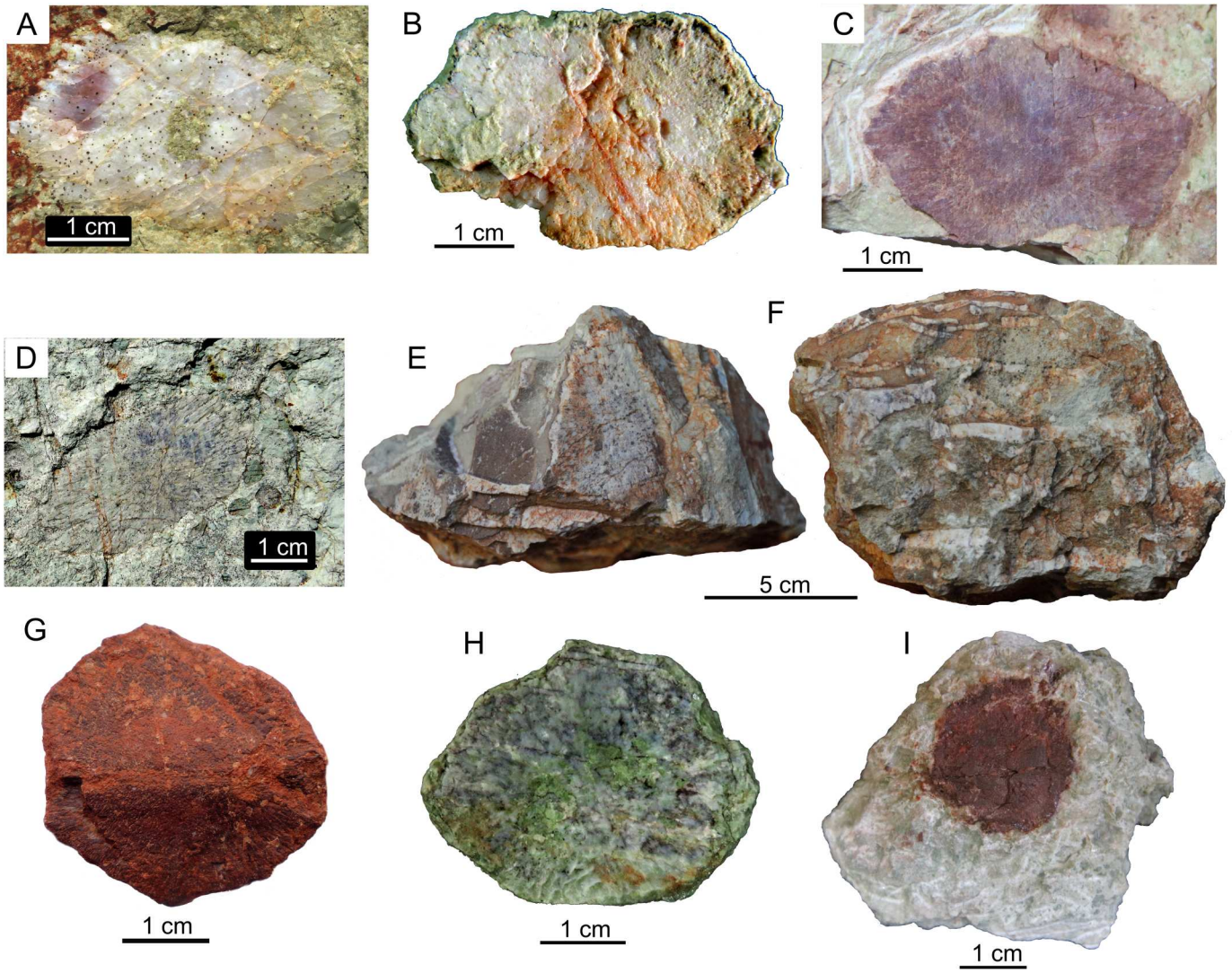

FIGURE 2. Cyamodontoid placodont dermal armor plates recovered from the Upper Triassic deposits of the Algarve Basin. **A–F**, hexagonal elongated armor plates assigned to Cyamodontoidea cf. *Henodus*. They refer to morphotype 1 discussed in the text, which exhibits similarity to plates from the central portion of the *Henodus chelyops* carapace. **A**, armor plate (FCT-UNL 719) from Rocha da Pena site. **B**, armor plate (FCT-UNL 715) from Rocha da Pena site. **C**, armor plate (FCT-UNL 630) from the Vale do Álamo site. **D**, armor plate of Cyamodontoidea cf. *Henodus* from Vale Vinagre was observed in an isolated limestone block. **E**, **F**, armor plates described by Palain (1976) from São Bartolomeu de Messines as stegocephalian, herein attributed to Cyamodontoidea cf. *Henodus* (MG specimen unnumbered). **G–I**, equilateral hexagonal armor plates assigned to Cyamodontoidea indet. referring to morphotype 2. **G**, armor plate (FCT-UNL 628) from Rocha da Pena site. **H**, armor plate (FCT-UNL 717) from Rocha da Pena site. **I**, armor plate from the block containing ML. A9182 from Vale do Álamo site.

accumulation of cyamodontoid placodont armor plates (Fig. 2E, F). One armor plate is well exposed within the limestone block and is characterized by distinct elongation, flat surface with pitting, and very faint radial striation, resembling other armor plates assigned to morphotype 1 (Fig. 2E). This better-exposed plate is slightly larger compared with other specimens studied, as the maximal diameter of the preserved part is 5.4 cm. The specimen is incomplete as it lacks a large portion of the armor plate's margin. Most other plates are embedded in the limestone block with only cross sections visible (Fig. 2F). These preserved fragments of armor plates exhibit larger thickness than other armor plates studied, with thickness ranging between 0.3–0.6 cm.

Most of the recovered dermal armor plates at all sites were found as isolated elements, collected either as specimens embedded within carbonate or carbonated mudstone rocks or at the surface of the outcrop. The exception is FCT-UNL 714, found in São Bartolomeu de Messines, which consists of a block of sediment with a large concentration of mostly fragmented armor plates and unidentified bone fragments of small dimensions, not exceeding 5 cm (Fig. 3A). The block has 89 bones, mostly armor plates. All bone plates are disarticulated. The most complete armor plate preserved in this block has a hexagonal shape, with 3.8 cm in length and 2 cm in width (Fig. 3B). Like other better-preserved specimens from morphotype 1, it presents a combination of straight as well as serrated margins, with the latter likely referring to interdigitating sutures. Most other fragments present an angular shape. Some of those specimens exhibit slight radial ornamentation. Most armor plates are in a sub-horizontal position, but some are inclined up to 45°. Considering the spatial distribution, number, and disarticulation of armor plates, it is likely that the bones in the accumulation represent hydrodynamically re-deposited elements coming from various individuals.

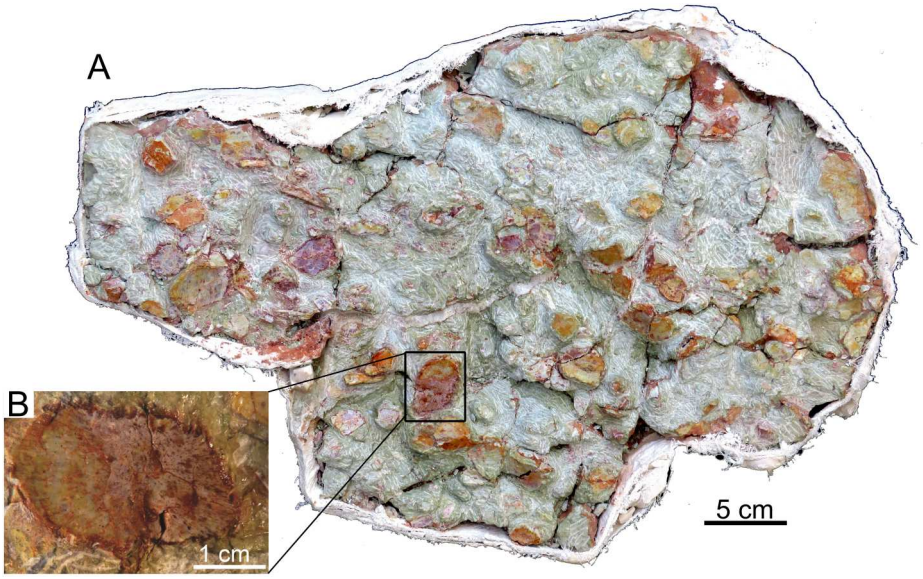

FIGURE 3. Block with a large concentration of cyamodontoid placodont armor plates and other undetermined bone fragments (FCT-UNL 714) from layer IC1722-2 of the stratigraphic section 1 observed in São Bartolomeu de Messines, municipality of Silves. **A**, photograph of the block FCT-UNL 714. **B**, close-up of one of the more complete armor plates from the FCT-UNL 714. This specimen is assigned to morphotype 1, thus referring to Cyamodontoidea cf. *Henodus*.

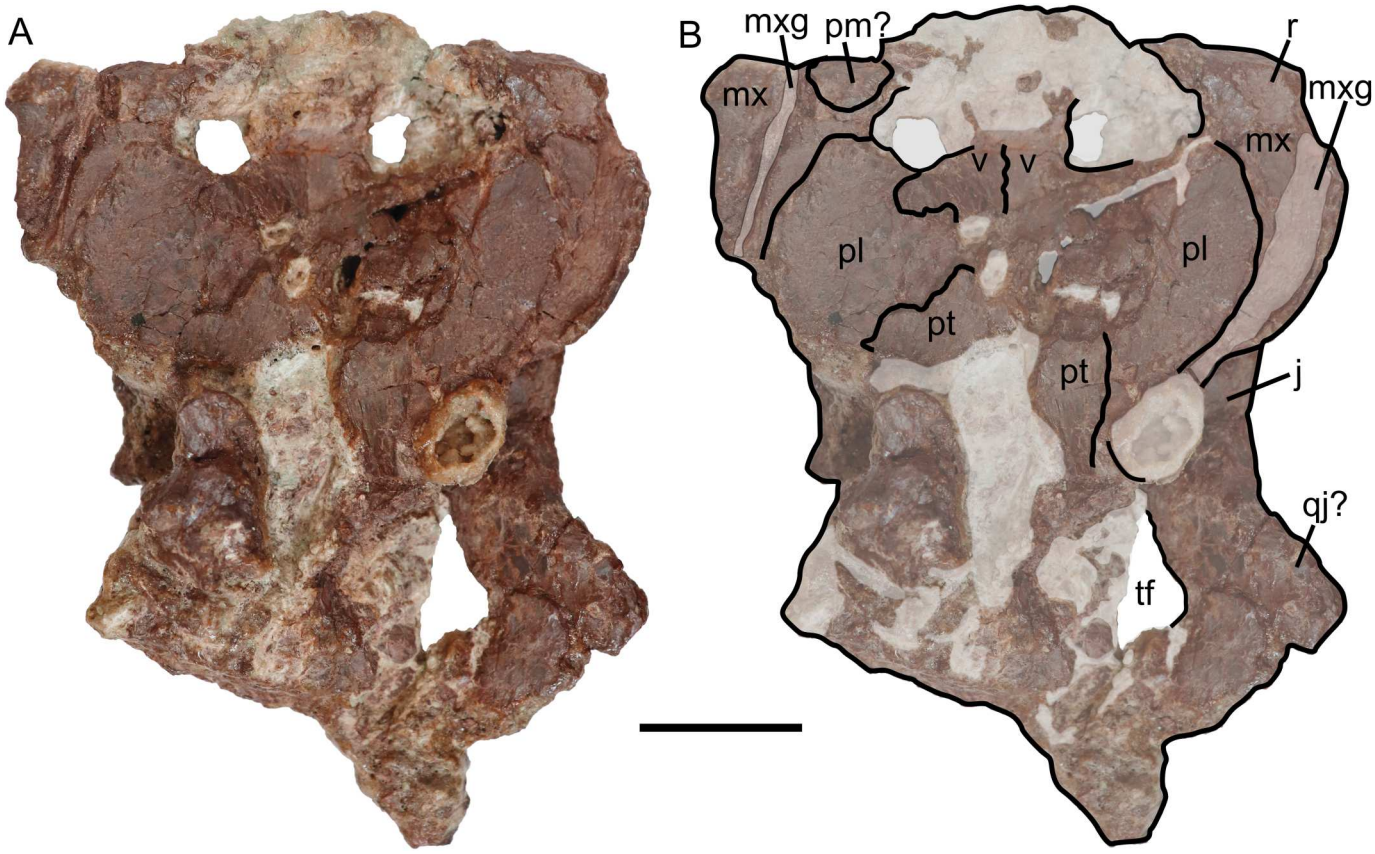

FIGURE 4. Cranium of *Henodus* sp. (ML. A9182) from the Late Triassic of the Algarve, southern Portugal. **A**, photograph in ventral view. **B**, same photograph with anatomical labels. **Abbreviations**: **j**, jugal; **mx**, maxilla; **mxg**, maxillary grove; **pl**, palatine; **pm**, premaxilla; **pt**, pterygoid; **qj**, quadratojugal; **r**, recess; **tf**, temporal fenestra; **v**, vomer. Scale bar equals 20 mm.

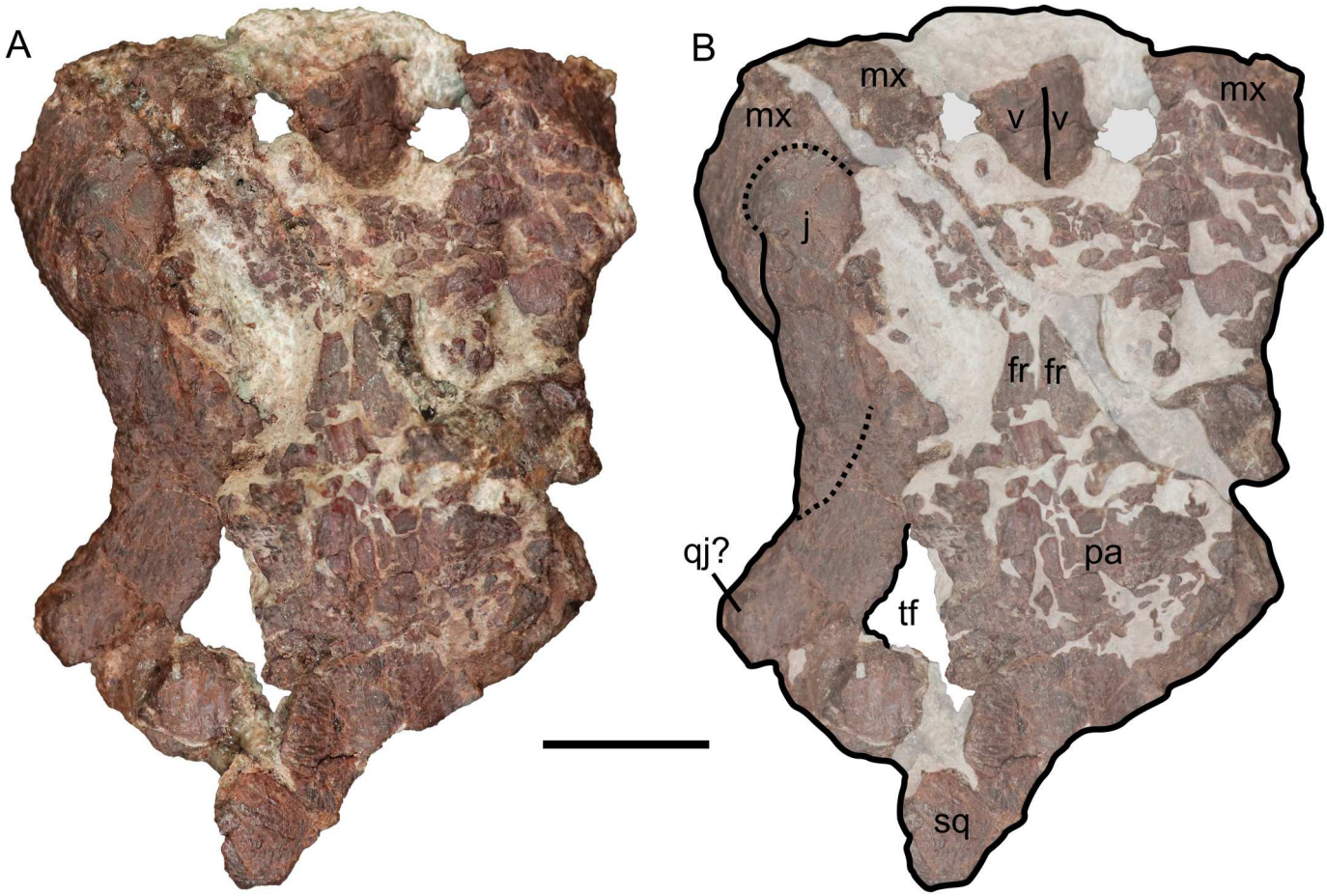

FIGURE 5. Cranium of *Henodus* sp. (ML. A9182) from the Late Triassic of the Algarve, southern Portugal. **A**, photograph in dorsal view. **B**, same photograph with anatomical labels. Straight line: established bone extension; dashed line: tentative bone extension. **Abbreviations**: **fr**, frontal; **j**, jugal; **mx**, maxilla; **pa**, parietal; **qj**, quadratojugal; ; **sq**, squamosal; **tf**, temporal fenestra; **v**, vomer. Scale bar equals 20 mm.

Comparison—The dermal armor plate material from the Upper Triassic of the Algarve is similar to cyamodontoid placodonts by the following characters: (1) hexagonal or heptagonal outline, (2) surface morphology varying from smooth to faintly marked ornamentation composed of minute foramina and radial groove and ridge pattern, (3) centimeter-sized plates, which do not excess 5 cm in diameter and are a few millimeters in thickness, and (4) in the case of the FCT-UNL 628, the occurrence of the low rounded keel occurring on bone plates as known from some placodont representatives (Rieppel, 2002b).

Although placodont armor plates may superficially resemble osteoderms of other tetrapods, previous histological studies indicate that they are most likely non-homologous structures (Scheyer, 2007; Scheyer and Klein 2021), at least on a macroscopic level. However, placodont armor plates can also be distinguished based on external morphology (e.g., de Miguel Chaves et al., 2020a; Rieppel 2002b).

Archosaurs represented by various groups, including phytosaurs, crocodylomorphs, and aetosaurs, possessed osteoderms with distinctly marked pit and ridge patterns, often with a pronounced well-developed keel (see works in Nesbitt et al., 2013). Those features are either lacking (pit and ridge pattern) or are much less developed (keel in some specimens) in the armor plates of placodonts. Moreover, archosaur osteoderms often differ from plates of placodonts in shape, usually having rectangular or oval outlines (see works in Nesbitt et al., 2013).

The other group, which possessed the bone plate at the time of the Triassic were early turtles. Scutes of turtles are distinct from the cyamodontoid osteoderms by either being polygonal, but at the same time usually largely irregular or distinctly elongated (de la Fuente et al., 2021; Gaffney, 1990; Szczygielski & Sulej, 2016). Most turtle dermal plates are distinctly larger than in the case of placodonts, only with some of the marginal ones possibly having approximate sizes (de la Fuente et al., 2021; Gaffney, 1990; Szczygielski & Sulej, 2016).

Saurosphargidae, a clade of highly discussed and uncertain phylogenetic position (Cheng et al., 2022; Li et al., 2014; Scheyer et al., 2017) and similar body construction to placodonts is also known to possess osteoderms (Cheng et al., 2022; Li et al., 2011, 2014; Scheyer et al., 2022; Wolniewicz et al., 2023). The osteoderms of saurosphargids display a wide range of morphology and sizes, varying both among species and among different regions of an individual's body. *Pomolispondylus biani* possesses bone plates covering neural spines, with the former exhibiting tuberous texture. Additionally, spindle-shaped bone plates are present along the sides of the gastralia rows (Cheng et al., 2022). The saurosphargid *Sinosaurosphargis yunguiensis* on the other hand has a well-developed carapace composed of numerous millimeter-sized, granular-shaped, and tubercule-like osteoderms, while *Largocephalosaurus kinesis* possesses rows of morphologically similar osteoderms, which do not form a carapace (Li et al., 2014). The latter also exhibits rows of larger osteoderms along the

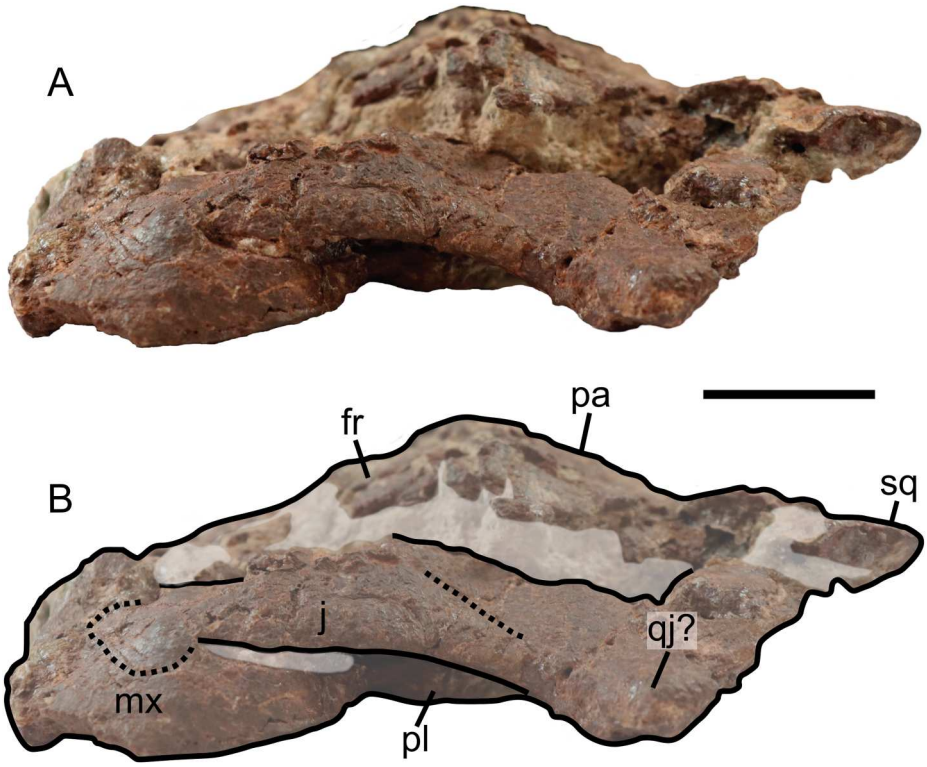

FIGURE 6. Cranium of *Henodus* sp. (ML. A9182) from the Late Triassic of the Algarve, southern Portugal. **A**, photograph in sinistral view. **B**, same photograph with anatomical labels. Straight line: established bone extension; Dashed line: tentative bone extension. **Abbreviations**: **fr**, frontal; **j**, jugal; **mx**, maxilla; **pa**, parietal; **pl**, palatine; **qj**, quadratojugal; **sq**, squamosal. Scale bar equals 20 mm.

dorsolateral surface of the body, associated with the ribs (Li et al., 2014). The Algarve armor plates can be readily distinguished from osteoderms of the outlined taxa by differing hexagonal and heptagonal shapes, larger sizes and smooth to faintly developed pitted and grooved textures.

Prosaurosphargis yingzishanensis on the other hand presents quite distinct osteoderm morphotypes, composed of centimeter-sized elongated, often irregular, sub-oval, or sub-rectangular bone plates with a densely pitted surface and a prominent ridge developed in some of them (Wolniewicz et al., 2023). Overall, *P. yingzishanensis* osteoderms can be distinguished from the better-preserved material from the Algarve by exhibiting a more irregular shape (lacking the regular hexagonal form), overall stronger pitting of the plates' surfaces, and/or an occurrence of the pronounced ridge (compared with faint and rather regular keel of equilateral armor plates from the Algarve).

Moreover, one of the bone plate types present in *Eusaurosphargis dalsassoi* shows similarities to the Algarve armor plates assigned to morphotype 1. *E. dalsassoi* is reported to possess a quite diverse bone plate morphology ranging from spindle, triangular, oval, to rectangular/shingle-like (Scheyer et al., 2017, 2022). The latter type presents slightly pitted, grooved, or smooth/platy surface textures, very similar to those observed in the Algarve material (see fig. 11b in Scheyer et al., 2017). The main clear difference can be observed in distinctly smaller sizes of the millimeter-sized *Eusaurosphargis* plates compared with prevalently 3–4 cm sized armor plates from the Algarve.

Therefore, the affinity of isolated armor plates from the Algarve to saurosphargids or of *Eusaurosphargis* cannot be entirely excluded, especially in the case of weakly preserved or incomplete specimens. Nonetheless, the Algarve material represents two morphological armor plate types regarding their size and shape, which are rather uncommon in saurosphargids or *Eusaurosphargis.* Moreover, the Algarve material lacks other forms of armor plate that are present in saurosphargids (e.g., elongated, oval, granular, and triangular forms). Based on those observations and due to the occurrence of the placodont cranial material described from the armor plate bearing stratigraphical layer, we consider assignation to Cyamodontoidea as the most parsimonious.

Placodont armor plates, which occur in association as a part of the carapace (or plastron) and/or exhibit very good preservation, may deliver taxonomic information, possibly up to the species level (Rieppel, 2002b). However, the precise taxonomic identification of the Algarve armor plates is restricted since the whole material is composed of isolated elements, mostly poorly preserved. The equilateral hexagonal or pentagonal plates with flat surfaces or having low keel and faintly marked radial ornamentation are present in multiple cyamodontoid taxa, including *Psephosauriscus*, *Cyamodus*, *Sinocyamodus*, *Psephoderma*, *Psephosaurus*, *Psephochelys* (Pinna & Nosotti, 1989; Rieppel, 2002b; Scheyer, 2010; Wang et al.,, 2019a, 2019b, 2020) and in the case of *Henodus chelyops*, they occur at the marginal portion of the carapace (Rieppel, 2002b; von Huene, 1936, 1938; Westphal, 1976). This illustrates a distinct degree of intraspecific morphological homogeneity and the common occurrence of this type of armor plate within Placodontia. This observation implies limited utility of taxonomic identification of those bone plates (when isolated) as already noted by de Miguel Chaves et al. (2020a, 2020b).

The laterally elongated armor plates represented by FCT-UNL 714, FCT-UNL 719, and FCT-UNL 715 show a morphology, which, so far, has been described in association only in the *H. chelyops* carapace. Those specimens especially resemble its medially placed M, a, b, and c-plates (von Huene, 1938), respectively. The Algarve specimens, as in the case of the mentioned

FIGURE 7. Photogrammetry-based 3D model of *Henodus* sp. (ML. A9182) cranium (image in sinistral oblique perspective, showing the dorsal side of the skull).

H. chelyops plates, have planar surfaces and exhibit both simple and straight, as well as interdigitating sutures. It is worth noting that similar elongated isolated armor plates assigned to Cyamodontoidea indet. were found in Carnian deposits of Manzanera located in eastern Spain (de Miguel Chaves et al., 2015).

ML. A9182—Description of Cranial Morphology

General Comments—ML. A9182 represents a cranial fragment, lacking the posterior and part of the lateral portions (Figs. 3–7, S6–S9). The skull was found embedded within the calcareous mudstone block and associated with an armor plate (Fig. S6S). It exhibits a poor state of preservation resulting from taphonomic alterations. It is broad, dorsoventrally flattened, and measures 10.3 cm in length. It is the widest at the level of the maxillae maximum lateral extensions, reaching a width of 7.9 cm. Approximately at the midpoint of the preserved cranium, it narrows and reaches its smallest width of 4.8 cm. Caudally to the midpoint of the skull, the posterior half broadens, resulting in an hourglass-like shape in the dorsal and ventral views.

Most of the skull table is highly taphonomically affected, especially its anterior half. The distortion is evident by numerous cracks and the fragmented nature of the preserved cranial elements, several of which are displaced (Fig. 5). A long, few millimeters thick crack extends obliquely throughout the skull, from the left anterolateral margin of the maxilla up to the narrowest area of the cranium. The area extending anterolaterally from the margin of the crack is characterized by a larger degree of bone fragmentation and distortion when compared with the posteriorly positioned part (Fig. 5).

In lateral view, the dorsal margin of the preserved skull is irregular but overall convex (Fig. 6). The exposed posterior half of the skull table presents a shallow dorsal extension, with the posterior margin being subtly inclined anterodorsally, dipping anteroventrally at the level of the mid-length of the skull. This upraised portion of the skull table constitutes the highest point of the cranium (2.5 cm). Most of the bones constituting the preserved skull table are distorted and rotated by ca. 30° from the original skull axis. Most of the ventral surface of the skull is sub-horizontal, only with the lateral process being inclined ventrolaterally.

Maxillae and Premaxillae—The anterior-most part of the preserved skull is composed of paired maxillae which constitute the anterolateral and anterior margins of the preserved cranium. The premaxillae are possibly represented by badly preserved small bone fragments contacting ventrally the anteromedial portion of the maxilla (Fig. 4). However, due to poor preservation and lack of clear original anatomical demarcation, identification of that element remains unsure, as it may also represent a ventral extension of the maxilla. Therefore, the whole or most of the premaxillae are missing in the specimen.

The left maxilla is almost complete, whereas the right one lacks a large part of its posterior portion. Even though the left maxilla is preserved, clear bone distortion occurs in its anteroventral part, near internal nares. In the dorsal view, the left maxilla expands on the anterior part of the skull, being posteriorly and medially constricted by the jugal (Fig. 5). The contact with the jugal is difficult to establish due to multiple cracks and lack of clear suture, thus the herein presented interpretation is tentative. Based on the spatial arrangement of bones, including the area of bone superimposition, the maxilla-jugal junction is herein interpreted to be characterized by a curved U-shaped margin (pointing anteriorly) in the dorsal perspective. In this interpretation, the anterior portion of the jugal incises and partly superimposes the medial portion of the maxilla. In the case of the right maxilla, the bone surface in the dorsal view is largely cracked and fragmented, hindering a more precise interpretation of bone extensions. Moreover, the posterior portion of the right maxilla is missing. Although the dorsal contact with the jugal is difficult to trace with confidence, the border between the two bones is demarcated ventrally (seen in the lateral perspective), whereas the left maxilla terminates ventromedially, resulting in the straight, sub-horizontal contacts of the maxilla and the overlying jugal.

This maxillary extension forms most of the lateral margin of the rostrum, expanding longitudinally to the narrowest point of the skull. In ventral view, the maxilla (well visible only in left view) is distinctly curved laterally, resulting in the convex shape of the lateral margins of the rostrum (Fig. 4). In ventral view, the maxilla is J-shaped, being laterally curved. In its anterior portion (anteriorly to the level of the internal nares) it is significantly expanded transversely, with the remaining portion gradually tapering posteriorly, terminating at the approximate level of the midlength of the cranial fragment. Within the anteriormost portion of the left maxilla, at the approximate level of the anterior internal nares' margin a small recess, a few millimeters in diameter, is visible. The smooth and rounded surfaces and edges suggest it represents the original feature and not a taphonomic alteration; however, its identification remains problematic at this point. The anterior part of the right maxilla extends medially, where it contacts the middle part of the lateral border of the internal nare. In the right counterpart, this morphology is not clearly defined due to the high degree of bone distortion in this area. Close to the right lateral margins of the maxilla, a maxillary groove is observed, which is well preserved only in the left maxilla. This maxillary grove is curved, half-moon shaped, and stretches throughout the almost whole length of the preserved part of the left maxilla. Its width is constant throughout most of its extension, drastically tapering within its posterior portion, near the point of maxilla termination. The maxillary groove is U-shaped in cross section.

The maxillary grooves (on both the left and right maxilla) are laterally and medially constricted by low ridges extending parallel to the groove. The lateral ridge is slightly more pronounced than the medial one, and dorsally, it terminates with a smooth, rounded surface. In the case of the right maxilla, only the anterior part of the groove is preserved (as the posterior part of the right maxilla is missing). This groove on the right maxilla appears to differ from the more posteriorly located (preserved) portion of a groove in the left maxilla by being more constricted and straight. Medially, the maxillae are confined by the palatines.

Vomers—The paired vomers extend at the anterior-most area of the medial part of the preserved cranium and are, in the skull fragment, visible from both ventral and dorsal perspectives. Anteriorly, the vomers almost reach the level of the maxillae anterior margin, while their maximal posterior extension and margin remain problematic to establish. The anterior and central portions of the vomers form a rectangular element with overall straight margins and clear demarcation between the two vomers. The division between the two bones is roughly straight and is noticeable throughout most of the anteroposterior extension of the vomers. In the ventral perspective, the central area of the vomers is concave, while its dorsal surface is subtly convex. At the level of the posterior internal nares' margins, the vomers expand laterally. Nonetheless, it can be only clearly noticed in the right vomer, because in the left counterpart, this skull area is highly distorted and cracked. The posterolateral protrusion of the right vomer extends approximately to the level of the mid-width of the internal nares. This protrusion is overall triangular and superimposes a small part of the anteromedial portion of the palatine. The part of the identified posterior vomer margin laterally contacts the palatine, while medially it contacts the bone fragments, which most likely constituted the anterior portion of the pterygoids. The lateral margins and posterolateral extensions of the vomers define the medial and part of the posterior borders of the internal nares (around half of the posterior internal margin, while the second half is formed by the palatine margins extending laterally to the vomers).

Palatines—The paired palatines stretching longitudinally near the lateral margins of the skull are separated by the vomers in their anterior-most portion and by the pterygoids in their middle and posterior parts. The left palatine is almost completely preserved, whereas the right one lacks a big posterior portion. While in the case of the left palatine the sutures between preserved bone elements can be identified, the medial margin of the left palatine is largely cracked and distorted and cannot be uncontestably determined. The preserved parts of both palatines have an overall oblong outline being also slightly laterally curved. They stretch parallel to the maxillae. The anterior margins contact the posterolateral margins of the internal nares as well as the posterolateral margins of the vomers. At the lateral margins, the palatines contact the maxillae and are separated from them by the subtly rounded ridge. The anteromedial borders of the palatines are confined by the vomers, although they can be only observed in the right portion of the skull. Medially in the more posterior portion, the palatines contact elements which are herein interpreted as the pterygoids, while more anteriorly the "extensions" are unidentifiable bone fragments. The latter, however, also most likely represent parts of the pterygoids, or in the anteriormost portion, fragments of the vomers. The preserved portion of the left palatine tapers approximately at the level of the minimal width of the skull. This portion of a palatine includes an oval carbonate geode, created during diagenesis. In the case of the right palatine, this area is not preserved. The palatines' surfaces are irregularly covered with small, millimeter-sized, shallow irregular polyhedral pits.

Pterygoids—The pterygoids are quite poorly preserved, with only small, isolated fragments, hampering any detailed description. The preserved fragments of the pterygoids are irregular and dispersed within the central area of the cranial fragment. Based on the preserved elements, it can be deduced that the pterygoids covered the medial section of the middle and posterior parts of the ventral side of the skull, anteriorly contacting the vomers, and laterally the palatines. However, the level of anterior extension of the pterygoids and their junction with the vomers remain problematic to establish. The surfaces of the fragmented pterygoids are locally covered by sparse, elongated shallow millimeter-thick grooves, differentiating them from other bones which are—in contrast—characterized by smooth or slightly pitted surfaces.

Cranial Lateral Margins—The left lateral margin of the skull is much better preserved than the right one. In the case of the latter, only the anterior portion is not damaged. Within the left lateral margin of the cranium, a complex of bones, most probably including maxilla, jugal, quadratojugal, and squamosal can be defined, while in the case of the right lateral margin bone(s) are either distorted or missing. The bone complex observed with the left lateral margin of the cranium forms a seemingly uniform element extending almost until the posterior margin of the preserved part of the skull. This element is broad and slender, dorsoventrally flattened, and slightly ventrally inclined with its surface being slightly concave.

Jugals—The anterior portion of the right jugal can be identified, as contacting the maxilla (although its precise extension and the dorsal jugal-maxilla junction are difficult to establish; see the description above concerning maxillary-jugal contact). Due to the occurrence of multiple cracks and grooves, which can seemingly appear as possible borders of the bones, the extension of the jugal remains highly speculative. We tentatively identified one distinct groove as the likely suture between the posterior portion of the jugal and bone material positioned more posteriorly (Fig. 6). It extends obliquely from the lateral margin of the cranium at the level of the start of the lateral process until the more dorsally oriented position of the bone, almost at the level of the minimal skull width. Such interpretation would result in the reconstruction of the jugal with a gradually posteriorly tapering process. The extension of the remaining portions of the jugal is even harder to establish.

Lateral Process—In the more posteriorly positioned portion of the cranium, a triangular-shaped process terminates the skull ventrolaterally, reaching the right maxilla's maximum lateral extension. It is possibly composed of quadratojugal, although bone extensions cannot be uncontestably determined in this area. Nonetheless, undoubtedly, it was confined posteriorly at some point by the squamosal, which could be represented by the identified partially isolated and fragmented elements of ML. A9182 described above. The medial margin within the area of the ventrolateral process constitutes the lateral margin of the temporal opening.

Temporal Fenestra— Only the left temporal opening is preserved, as ML. A9182 misses a large portion of the right lateral margin. The preserved temporal fenestra has an irregular but overall triangular shape. Its medial margin is damaged and irregular, but overall straight. It is defined by a highly bone-cracked area in the anterior portion and by the parietal in the middle and posterior parts. The posterior-lateral margin of the opening constitutes the largely cracked parts of the squamosal. The lateral margin of the opening is defined by a triangular-shaped process, possibly composed of the quadratojugal. The medial margin of this process, which forms the lateral margin of the opening, is represented by unaltered and well-preserved bone, suggesting that the opening represents an original morphological feature rather than a taphonomic artifact. The remaining edges are rather irregular, characterized by a high degree of breakage and jagged surfaces.

Skull Table—The posterior area of the skull table is upraised and slightly dorsally inclined. The preserved skull table forms a rectangular-like outline with posterolateral termination (Fig. 5). Most of the central area of the skull roof is likely composed of the parietal; however, the occurrence of other bone fragments in the studied specimen (e.g., postorbital, postfrontal) can be neither excluded nor confirmed. The posterolateral termination is composed of a part of the squamosal. The preserved part of the parietal is broad, although its outline is hard to interpret. Undoubtedly, the parietal constitutes most of the posterior margin of the preserved cranium. To the left lateral margin of the distal part of the parietal, two fragments of a squamosal extend, but at the more ventrally extending plain in regard to the parietal. Anteriorly to the parietal area, highly fragmented bones occur, which possibly constitute parts of the postorbital, postfrontal, and frontal.

At the level of the maximal height of the skull tables, resulting from its dorsal inclination, the preserved skull roof bones abruptly dip ventrally. Fragments of the possibly posterior part of the paired frontal can be identified within this area. The fragment is longer than wide and narrows anteriorly. Anteriorly and laterally, the fragments of the frontals contact the area covered with highly fragmented bones. The surface covered with those bones diverges almost at the level of the anterolateral margin of the orbits, giving the Y-like shape to this association of bone fragments (Figs. 5, 7). This bone association extends anteriorly until it contacts the maxillae, near the anterior margin of the skull. Based on the observations of the specimen, it is impossible to assess with certainty which bones are included in this accumulation. However, while comparing the better-preserved left margin of the specimen, it can be assumed that the area extending throughout the right margin was probably composed of the maxilla (at the anterior portion) and the jugal (at the posterior part). The more medial and the anterior areas can be possibly composed of fragments of the postorbital, frontal, and prefrontal, although none of those bones can be identified uncontestably. Moreover, due to the noted deformations, the outlines of the nares and orbits cannot be traced. At the anteromedial area of the skull, a fragment of the vomer is exposed. It is rectangular, with slightly irregular but mostly straight margins. Its medial part is cut by a longitudinally extending shallow furrow.

ML. A9182–Comparison

General Comments—The cranium specimen ML. A9182 exhibits the square-shaped and significantly dorsoventrally flattened skull with a well-developed spatulate rostrum, which is relatively uncommon among tetrapods. Only two Triassic taxa with such a morphology were recovered, *Atopodentatus unicus* from the Anisian of China (Chun et al., 2016) and *Henodus chelyops* from the Carnian of Germany (von Huene, 1936).

Comparison to *Atopodentatus unicus*—ML. A9182 is similar to *Atopodentatus unicus* in terms of (1) an overall rectangular-like shape of the skull, (2) a distinct dorso-ventral compression of the cranium, (3) a well-developed rostrum, and the general arrangement of bones within the ventral part of the cranium with (4) palatines separated by long pterygoids, which contact the vomers, (5) elongated palatines contacting the maxillae laterally along the whole bone extension, and (6) contacting the pterygoids medially at their middle and posterior portion.

However, when considered in detail, the morphology of ML. A9182 deviates from *A. unicus* as follows: (1) ML. A9182 has a more hourglass-like shape compared with the more constricted cranium of *A. unicus*. (2) Although lacking the premaxilla, the rostrum of ML. A9182 was more likely spatulate compared with the T-shaped rostrum of *A. unicus*. (3) In ML. A9182, the palatines are broad and curved reaching the level of internal nares and participating exclusively in the posterior margin of internal nares compared with the palatines of *A. unicus* being straight and slender and extending beyond the level of anterior margin of the internal nares and participating in their posterior and lateral margins. (4) The maxillae of ML. A9182 are J-shaped and much broader compared with the right-angle L-shaped and slender maxillae of *A. unicus*. (5) There is a broad contact along the anterior margin of the jugal with the maxilla in ML. A9182 with a more posteriorly oriented anterior margin of the jugal being separated from the maxilla by broad vomers. (6) There are toothless maxillae in ML. A9182, but maxilla with multiple needle-shaped teeth in *A. unicus*. (7) ML. A9182 maxillae are massive at their anterior margin and not distinctly extending laterally in regard to more posteriorly located portions of the skull, compared with *A. unicus* with very slender and significantly laterally expanded maxillae in their anterior portions. Those morphological differences combined with distinctly different temporal and geographic range of *Atopodentatus*, decisively indicate the taxonomic distinctiveness of ML. A9182 and *A. unicus*.

Comparison to *Henodus chelyops*—There are two major, partly discrepant, interpretations of skull bone extensions of *Henodus chelyops* presented in the works of von Huene (1936), Rieppel (2001, 2002a) and Rieppel et al. (2000). The herein-presented comparison with *H. chelyops* is based on interpretations proposed by Rieppel (2001, 2002a) and Rieppel et al. (2000), as they largely align with our personal observation of the specimens.

ML. A9182 exhibits multiple similarities to *H. chelyops*: (1) flat and broad skull, (2) an overall elongated shape of the skull in dorsoventral view, (3) a short, broad, and spatulate rostrum, (4) J-shaped maxillae in the ventral view, (5) maxillae without teeth, (6) maxillary dentition substituted by a deep, longitudinally extending curved groove, which is U-shaped in transverse section, (7) a sub-horizontal, elongated maxillary-jugal contact along the ventral termination of the maxillae, located in the anterior portion of the cranium, (8) possibly a U-shaped dorsal junction between the maxillae and the jugals, with the latter partly superimposing posterior part of maxillae, (9) non-contacting, elongated, and broad palatines separated by the pterygoids and the vomers, (10) the palatines distinctly tapering in the posterior portion at the level of maxilla termination, (11) large internal nares separated by vomers, (12) palatines forming at

least half of posterior internal nares margin, (13) maxillae participating in the lateral margins of the internal nares, (14) the elongated, slightly ventrally inclined slender lateral margin of the cranium with the terminating triangular process at the level of the parietal, and (15) a broad and extensive parietal occupying a significant portion of the central and posterior area of the skull table. Therefore, most of the recognized bones in ML. A9182 (pertaining to the maxilla, jugal, palatine, vomer, parietal, and parts of frontal and squamosal) have a generally similar position, shape, and spatial arrangement when compared with *H. chelyops*.

Moreover, the resemblance between ML. A9182 and *H. chelyops* can be observed in less evident features, such as a similar flexure of the vomers in their central portion, the occurrence of a rounded recess in the anterior-most portion of the maxilla, and the surface morphology of the pterygoids composed of longitudinal striation (obs. pers., 2023; see also von Huene, 1936; Rieppel, 2001). The left temporal opening present in ML. A9182 is also similar to those seen in some *H. chelyops* specimens (obs. pers., 2023; Rieppel, 2001). The study of seven specimens of *H. chelyops* stored in Paläontologische Sammlung der Universität Tübingen (acronym: GPIT), Germany, revealed a great plasticity in both original morphology and preservation of the temporal opening, including closed temporal fenestrae (GPIT-PV-30006), a vestigial condition or depression within the covering parietal (GPIT-PV-30002), an opening in form of taphonomic artifact (GPIT-PV-30004), open temporal fenestrae, but not preserved in original shape due to breakage (GPIT-PV-30001 and GPIT-PV-30002), and well-preserved temporal fenestrae (GPIT-PV-30007). The original condition of temporal fenestrae in ML. A9182 remains unsure due to significant breakage of the skull table, which forms the medial margin of the opening. However, the morphology of the rounded lateral margin suggests the original presence of the opening. Thus, in ML. A9182, an open or vestigial original condition of temporal fenestra appears to be most likely. Regardless of the interpretation, the opening in ML. A9182 closely resembles conditions seen in *H. chelyops* (especially in the best-preserved specimens GPIT-PV-30003 and -30007), which can be noted by its position laterally to the parietal and at the level of the lateral process, a relatively small size, and a similar shape of its preserved lateral margin (obs. pers., 2023; see figures in Rieppel, 2001).

The skull table of ML. A9182 is badly preserved, impeding detailed comparison. Nevertheless, the preserved part of the parietal is broad and appears to broaden posteriorly, resembling the condition of a fan-shaped parietal occurring in *H. chelyops* (Rieppel, 2001; Rieppel et al., 2000; von Huene, 1936).

ML. A9182 is of comparable but moderately smaller size compared with *H. chelyops* specimens. This can be noted for example in the (maximal) width of the (almost complete) rostrum of ML. A9182 consisting of 7.9 cm compared with a range of 9.43 cm (GPIT-PV-30002) to 10,82 cm (GPIT-PV-30006) seen in skulls of *H. chelyops*. Overall, the recognizable skull portions of ML. A9182 appear to be ca. 20–30% smaller when compared with *H. chelyops*.

The only unambiguous morphological differences between ML. A9182 and *H. chelyops* pertain to the robustness and detailed skull shape. ML. A9182 has a broader rostrum with more rounded margins, resulting in a more robust appearance of the anterior portion of the skull compared with *H. chelyops*. In *H. chelyops*, in all recovered skulls the rostrum margins formed by the maxillae are either constricted and straight or subtly convex (von Huene, 1936, 1938; Rieppel, 2001), conversely to distinctly convex margins in ML. A9182. Compared with *H. chelyops*, the mid-length portion of the maxilla in ML. A9182, approximately at the level of the posterior margin of internal nares, has a much wider lateral extension and terminates laterally up to the maximal lateral extension of the lateral process likely formed by the quadratojugal. In *H. chelyops*, the respective area of the maxilla reaches laterally only the base of the mentioned lateral process, while the level of the maximal lateral extension of the process is reached by the anterior-most part of the maxilla (von Huene, 1936; Rieppel, 2001). The lateral process of ML. A9182, most likely composed of quadratojugal, also appears to have a relatively further lateral extension than in the case of *H. chelyops*. The above-mentioned features result in a more hourglass-like shape of ML. A9182 compared with the more rectangular skull outline of *H. chelyops*.

The ventral surface of ML. A9182 is flat with most of the bones extending at a similar horizontal level, whereas in ventral view the skull of *H. chelyops* is dorsally curved (see figures in Rieppel, 2001). Considering the distinct distortion of ML. A9182 skull table and many bones forming the ventral portion of the cranium, it is possible that the skull has been compacted and its curvature could have been reduced. Thus, it is not fully clear if this feature constitutes the original (and thus different) morphology or taphonomic alteration.

Similarly, the lack of preserved palatine teeth remains ambiguous. The occurrence of the oval geode within the palatine in the respective place of such teeth in *H. chelyops* may suggest the occurrence of one palatine tooth in ML. A9182, which would be equivalent to the condition present in *H. chelyops* (Rieppel, 2001; Rieppel et al., 2000; von Huene, 1936). However, as the tooth itself is not preserved and we cannot observe any clear evidence of the occurrence of alveoli, the occurrence of this feature may not be confirmed, but as this region has been diagenetically altered, its presence cannot be excluded.

PHYLOGENETIC ANALYSIS

The phylogenetic analysis (Analysis 1) based on the diapsid matrix of Wang et al. (2022) resulted in 140 trees with 790 steps (CI = 0.294; RI = 0.683,0; RC = 0.201). The topology of the consensus tree (Figs. 8, S14, S15) is largely consistent with the results obtained by Wang et al. (2022). However, few significant differences were noted, pertaining to more cases of unresolved relationships in our analysis (Fig. S14), especially within Ichthyosauromorpha and, to a lesser degree, within Eosauropterygia, with few taxa nested in a slightly different part of the tree (e.g., *Wumengosaurus* and *Qianxisaurus*). After the application of resampling, the consensus tree resulted in better-resolved relationships within Ichthyosauromorpha but not in Eosauropterygia (Fig. S15). In the consensus tree, ML. A9182 is recovered within Henodontidae, as a sister taxon to *Henodus chelyops*. However, this position is supported by a rather low bootstrap value (22). Henodontidae incorporating *Parahenodus atancensis*, *Henodus chelyops*, and ML. A9182 are characterized by one synapomorphy—frontals paired (ch. 21; state 0), while ML. A9182 and *H. chelyops* are also distinguished by the depressed temporal region of the skull (ch. 41; state 0).

All the scored character states for ML. A9182 are consistent with conditions stated for *H. chelyops* (ch. 3; state 0; ch. 21; state 0; ch. 29; state 0; ch. 34; state 0; ch. 41; state 1; ch.62; state 1; ch. 64; state 0; ch. 65; state 0; ch. 89; state 1; ch. 179; state 0).

The phylogenetic analysis (Analysis 2) based on the diapsid matrix of Wang et al. (2019a) modified from Neenan et al. (2015), including ML. A9182 (Supplementary File 4), resulted in 20 most parsimonious trees, with a length of 610 steps (CI = 0.316; RI = 0.694; RC = 0.220). The topology of the consensus tree (Fig. S16) is consistent with the results obtained by Wang et al. (2019a). After the application of resampling, the consensus tree attains a slightly different topology, resulting in the better-resolved placement of taxa within Sauropterygia (Fig. S17). Otherwise, the changes are minimal and do not impact interpretations for this study.

In the consensus tree ML. A9182 is recovered within cyamodontoid placodonts as a sister taxon to *Henodus chelyops*. This

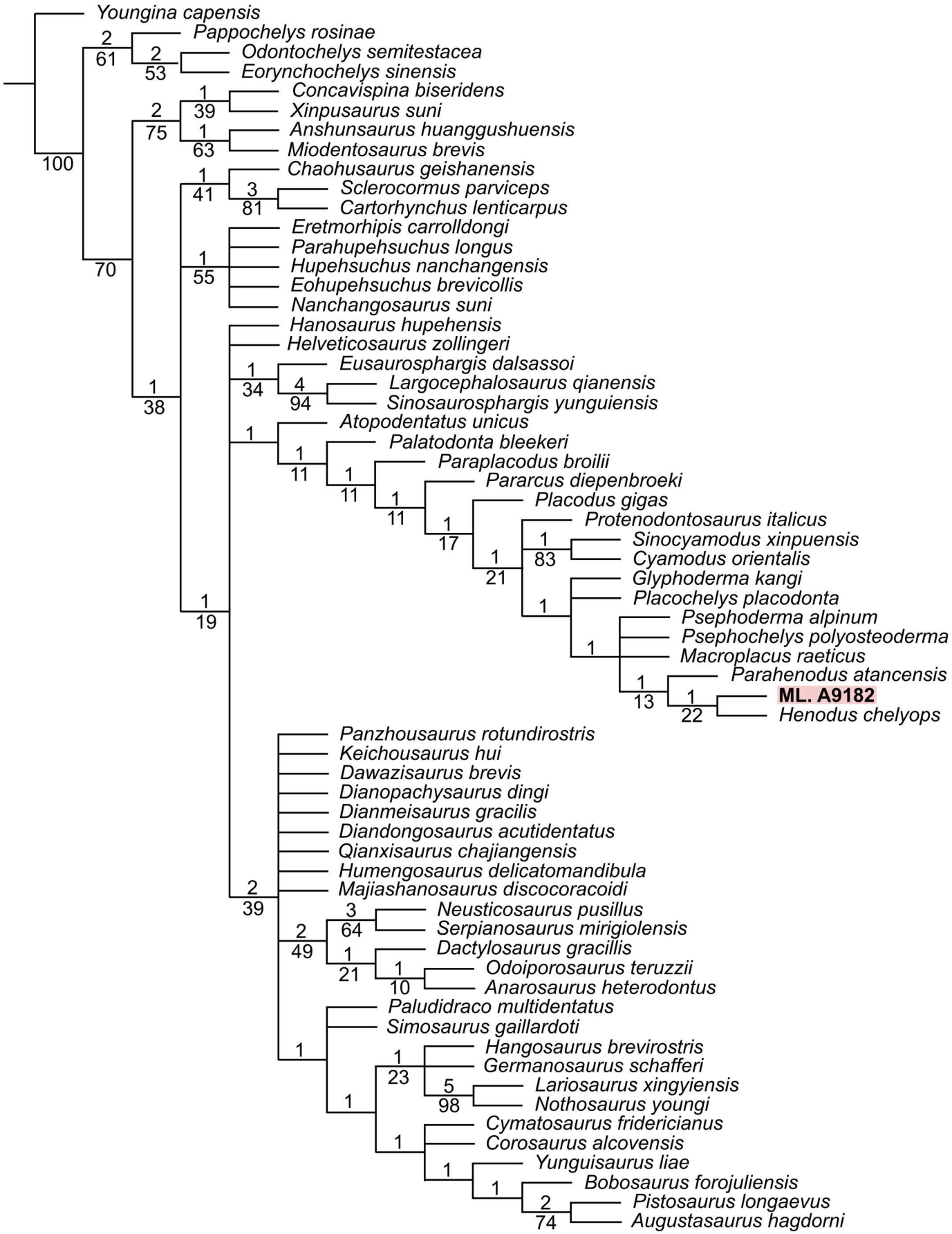

FIGURE 8. Strict consensus tree obtained from parsimony phylogenetic analysis using the diapsid character data matrix of Wang et al. (2022), with indication of the recovered position of ML. A9182 (*Henodus* sp.) from the Upper Triassic of Algarve. Bremer values are indicated above the nodes, while bootstrap values (≥ 10) are presented below the nodes.

position is supported by a relatively high bootstrap value (76). Henodontidae incorporating ML. A9182 and *H. chelyops* presents the following synapomorphies: short snout (ch. 3; state 2); depressed temporal region of the skull (ch. 28; state 1) and absence of maxillary tooth row, which is substituted by longitudinal furrow (ch. 68; state 3). All the scored character states for ML. A9182 are consistent with the conditions stated for *H. chelyops* (ch. 3; state 0; ch. 15; state 0; ch. 19; state 0; ch. 23; state 0; ch. 28; state 1; ch. 48; state 1; ch. 50; state 0; ch. 67; state 1; ch. 68; state 3; ch. 139; state 0). However, it should be noted that due to incompleteness and taphonomic alterations of ML. A9182, only 10 out of 140 characters were scored.

The phylogenetic analysis (Analysis 3) based on the original non-revised matrix of Neenan et al. (2015) with an extension using *Parahenodus atancensis* and ML. A9182 resulted in five most parsimonious trees, with a length of 135 steps (CI = 0.570; RI = 0. 663; RC = 0.378). The topology of the consensus tree (Fig. S18) is comparable to the obtained tree based on revised scoring. The major difference pertains to the better resolved relationships within Cyamodontoidea. However, after bootstrap applications, consensus tree topology is identical to the one based on the revised scoring (Fig. S19).

The phylogenetic analysis (Analysis 4) based on the matrix of Neenan et al. (2015), with the revised characters for *Henodus chelyops* and extensions using *Parahenodus atancensis* (de Miguel Chaves et al., 2018a) and ML. A9182 resulted in six most parsimonious trees, with a length of 135 steps (CI = 0.570; RI = 0.667; RC = 0.380). The topology of the consensus tree (Fig. S20) is consistent with the results obtained by Neenan et al. (2015) and de Miguel Chaves et al. (2018a); however, two differences appear after the application of bootstrap calculation. First, instead of a polytomy within Cyamodontida, the Cyamodontidae (composed of *Sinocyamodus xinpuensis* and all species of *Cyamodus*) and Henodontidae are recovered as monophyla (Fig. S21). Moreover, *Protenodontosaurus italicus* is placed outside of Placochelyida, being part of a polytomy with Placochelyida and Cyamodontida, located within Cyamodontidae.

In the consensus tree ML. A9182 is recovered within Cyamodontida as a part of Henodontidae and placed in the unresolved group containing *Henodus chelyops* and *Parahenodus atancensis.* However, after the application of bootstrap calculation, the topology of Henodontidae changes, resulting in a breakage of the polytomy and placement of *P. atancensis* outside of *H. chelyops* and the ML. A9182. This separation is, however, only supported by a very low bootstrap value of 3 (Fig. S21).

Compared with most other placodont clades, the placement of ML. A9182 within Henodontidae is supported by the relatively high bootstrap of 63 (Fig. S21). Henodontidae recovered in the presented analysis comprises the following synapomorphies: short snout (ch. 3; state 2); the absence of maxillary teeth but the presence of a longitudinal maxillary furrow (ch. 35; state 4); palatines are at least partially separated by long pterygoids (ch. 60; state 0). Another synapomorphy of Henodontidae indicated in previous studies (de Miguel Chaves et al., 2018a; Neenan et al., 2015), refers to the one pair of palatine teeth (ch. 36; state 3), which cannot be uncontestably determined in ML. A9182. However, this feature might have been also present in the ML. A9182 as the carbonate geode could be a recrystallized alveolus. All the scored feature states for ML. A9182 are consistent with conditions stated for *H. chelyops* (ch. 3; state 2; ch. 35; state 4; ch. 39; state 1; ch. 42; state 0; ch. 60; state 0).

The obtained topology and position of ML. A9182 as a sister taxon to *H. chelyops* in all conducted analyses may support the identification of ML. A9182 as belonging to the genus *Henodus.* However, these results should be treated with large caution as only a small portion of characters were possible to be scored. Therefore, the obtained results may be impacted by the substantial incompleteness of the feature scoring.

DISCUSSION

Dermal Armor Plates—Taxonomic and Chronostratigraphic Implications

The armor plate material from the Algarve sites is attributed to cyamodontoid placodonts, based on their overall hexagonal or heptagonal shapes, smooth to pitted and subtly striated surface, and small size and thickness (sensu de Miguel Chaves et al., 2020a; Rieppel 2002b). Some material, especially represented by the elongated bone plates, resembles the armor plates placed in the medial portion of the carapace of *H. chelyops* (von Huene 1936, 1938). Therefore, in the scope of morphological similarity and—based on the cranial material (see below)—the confirmed occurrence of *Henodus* in the Algarve, it is possible that the elongated hexagonal armor plates belonged to *Henodus.* The equilateral plates may also belong to a henodontid placodont, but possibly stem from different portions of the carapace (Fig. 9), perhaps the marginal area as seen in *H. chelyops* (von Huene 1936, 1938). This assumption can be supported by the fact that the specimens were recovered from the same layers as the elongated hexagonal osteoderms and ML. A9182 cranium. However, due to the large morphological homogeneity of the placodont bone plates (de Miguel Chaves et al., 2020a, 2020b), uncontested identification of this material is not possible. Therefore, we assign armor plates of morphotype 1 as Cyamodontoidea cf. *Henodus*, as this plate morphology has been so far known in this genus, while specimens of morphotype 2 are attributed to Cyamodontoidea indet.

Placodont armor plates, typically as fragmentary specimens, occur commonly across multiple horizons within the investigated sites. Notably, within these layers, placodont fossils stand out as the only identifiable tetrapod remains (Ruciński, 2020). This observation may correspond to sampling bias, taphonomic processes influencing the re-deposition of fossils (e.g., selective hydrodynamic sorting of placodont remains), a distinctly large number of plates in the carapace increasing their likelihood of preservation and recovery, an inherent abundance of placodonts in the area alongside a low diversity of other faunal components, or a combination of these factors. Regardless of the interpretation, the numerical abundance of armor plates and their occurrence across multiple stratigraphic levels and sites suggest that placodonts occurred commonly in the discussed region, likely constituting a significant component of the local fauna during the Late Triassic.

Taxonomy of ML. A9182

ML. A9182 is identified as a fragment of a cranium, exhibiting affinity to representatives of Henodontidae, especially to *Henodus chelyops.* Some of the most diagnostic cranial features of henodontid placodonts (de Miguel Chaves et al., 2018a; Rieppel, 2001; Rieppel et al., 2000) are present in ML. A9182, such as the lack of maxillary teeth, which are instead substituted by a maxillary furrow, and the separation of the elongated palatines by the pterygoids. The size-reduced pair of palatine teeth characteristic of henodontid placodonts (de Miguel Chaves et al., 2018a; Rieppel, 2001; Rieppel et al., 2000) is not observed in ML. A9182. However, as in the corresponding area to the Henodontidae palatine tooth alveolus, ML. A9182 is covered with a carbonate geode of comparable size to henodontid teeth, the original condition could have been altered due to diagenesis. ML. A9182 shares the abovementioned features with the other known henodontid placodont: *Parahenodus atacensis.* Nonetheless, ML. A9182 can be distinguished from the latter by the rectangular-shaped skull and spatulate broad rostrum. *Parahenodus atacensis* exhibits a plesiomorphic, anteriorly tapering rostrum, characteristic of other cyamodontoid placodonts (de Miguel Chaves et al., 2018a, 2020c).

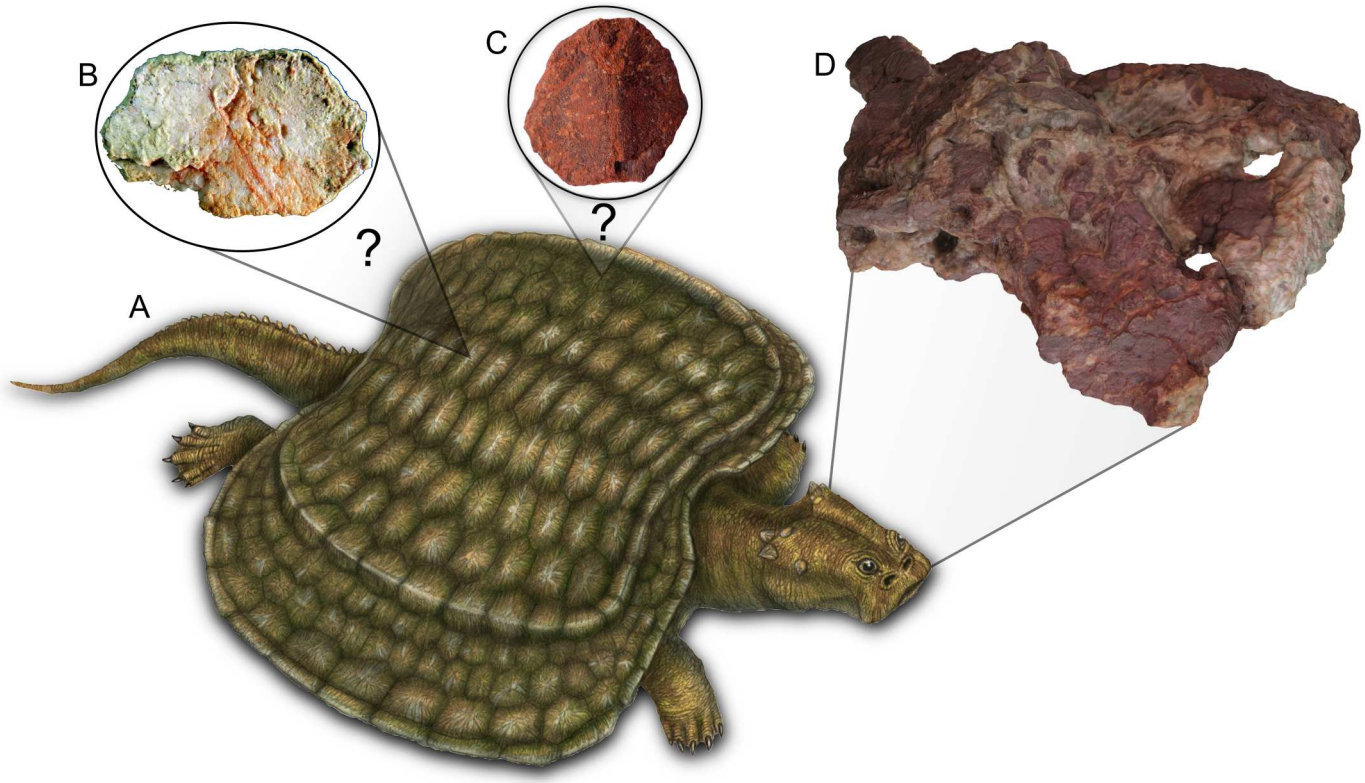

FIGURE 9. Summary of the placodont material from Upper Triassic of the Algarve. **A**, reconstruction of *Henodus* by Jakub Kowalski and Piotr Janecki. **B**, transversely expanded armor plate from Algarve, interpreted to possibly stem from the medial portion of *Henodus* carapace. **C**, equilateral armor plate from the Algarve interpreted to possibly stem from the marginal portion of *Henodus* carapace. **D**, photogrammetry-based image of *Henodus* cranium (ML. A9182).

Beyond the outlined characters, ML. A9182 shares multiple other features with *H. chelyops*, including the generally rectangular shape of the cranium, comparable placement of the preserved bones, as well as their shape and spatial arrangement. The only clear morphological difference between ML. A9182 and *H. chelyops* pertains to the more rounded and robust rostrum of ML. A9182, which results in a more hourglass-like shape of the specimen. As ML. A9182 does not exhibit any other significant morphological differences to *H. chelyops*, the distinct shape of the ML. A9182 and its smaller size can be considered within both scenarios of interspecific differences as well as intraspecific variation within *H. chelyops.*

The significant intraspecific variability in cranial geometry, including snout shape, commonly occurs in both extant and extinct sauropsid species, e.g., in the turtles *Apalone* ("*Trionyx*") *ferox* (Dalrymple, 1977) and *Trachemys dorbigni* (Portela et al., 2020), as well as in the eusuchians *Melanosuchus niger* (Foth et al., 2015) and *Allodaposuchus precedens* (Martin et al., 2016), among many other taxa. The intraspecific morphological variability depends on the ontogenetic stage but also polymorphism including sexual dimorphism and geographic distribution (Clark, 1976; Wiens, 1999). Notably for the studied case is that *H. chelyops* exhibits intraspecific morphological plasticity, which also pertains to the rostrum shape (obs. pers., 2023; Rieppel 2001). Some specimens (e.g., GPIT-PV-30001 and 30002) are characterized by straight and constricted rostrum margins, while in the case of others (e.g., GPIT-PV-30006, -30007), the margins are very subtly rounded and convex, although to a significantly much smaller extent than seen in ML. A9182 (obs. pers., 2023; see also figures in Rieppel, 2001). This illustrates the morphological variability exposed by only a few specimens of similar size and derived from the same place and stratigraphic level. Based on those observations as well as the lack of a larger number of morphological differences, we consider, for now, the variation in the observed snout shape and size of ML. A9182 might have been possibly driven by intraspecific variation within *H. chelyops* (i.e., ontogenetic stage, sexual dimorphism, or morphological variation between different populations).

Alternatively, the observed differences in snout shape and size in ML. A9182 may be interpreted within the context of representing a novel species. Such consideration could also be taken into account concerning the distinct distance between the area of southern Portugal and southern Germany during the Late Triassic (for different paleogeographic reconstructions see e.g., Golonka, 2007; Scotese & Schettino, 2017; Stampfli & Borel, 2002; Zeh et al., 2021). Moreover, ML. A9182 possibly represents a stratigraphically younger specimen compared with the early (or potentially middle) Carnian *H. chelyops* from Germany, as the minimal age of the stratigraphic unit where it was found is preliminarily constrained (see below) to be at least upper Carnian (Vilas-Boas et al., 2024). Thus, possibly making ML. A9182 at least several million years younger than the German specimens. The combined morphological, paleogeographic, chronological, and paleoenvironmental data indicating an inhabitation of somewhat restricted coastal settings (see below), suggest that a scenario involving the existence of a hypothetical second *Henodus* species cannot be excluded.

Unfortunately, the examination and verification of the outlined competing hypotheses are strongly hindered by the incompleteness and poor preservation of ML. A9182, hampering a

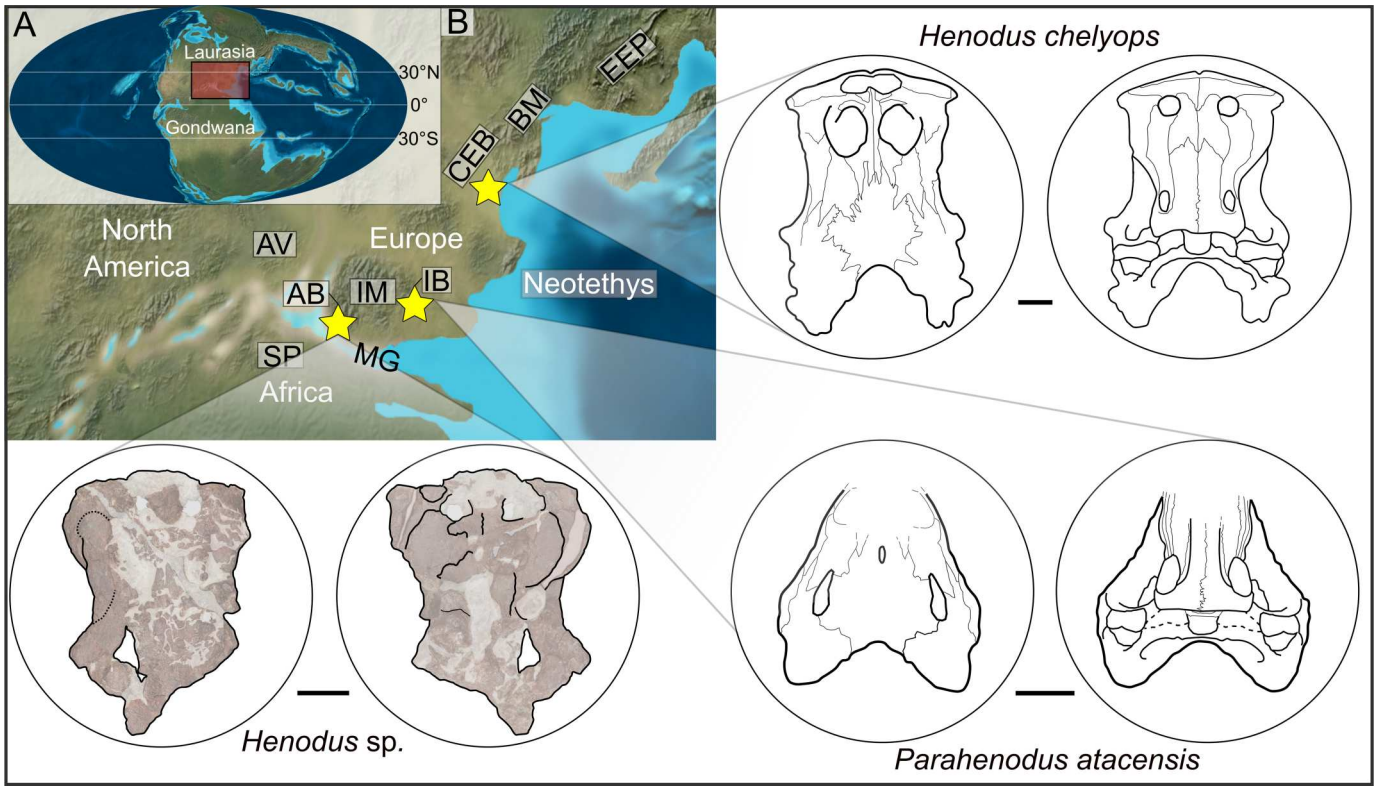

FIGURE 10. Paleogeographic context of recorded Henodontidae remains. **A**, paleogeographic map of the world during the Late Triassic (Colorado Plateau Geosystems Inc., license nr. #110719). **B**, magnification of the map of the Late Triassic world illustrating the area of the western Neotethys. Approximate locations of Henodontidae-bearing sites are indicated by a star. Drawing of *Henodus chelyops* after Rieppel et al. (2000). Drawing of *Parahenodus atacensis* after de Miguel Chaves et al. (2018a). Photos of the Portuguese specimen ML. A9182 is referred to as *Henodus* sp. with shape contour and established bone extensions (compare with Figs 4, 5). Scale bars represent 20 mm. **Abbreviations**: **AB**, Algarve Basin; **AV**, Avalonia; **BM**, Bohemian Massif; **CEB**, Central European Basin (which includes Germanic Basin); **EEP**, East European Platform; **IB**, Iberian Basin; **IM**, Iberian Massif; **MG**, Maghrabian-Gibraltar rift; **SP**, Sahara Platform.

comprehensive comparison to *H. chelyops*. Moreover, interpretations of the bone sutures in *H. chelyops* are also constrained by a varying preservation of cranial bones and sutures (Rieppel, 2001). Additionally, the chronostratigraphic constraints of the deposits containing ML. A9182 remain ambiguous, as palynological samples from those sections turned out to be sterile. Thus, the preliminary age constraint (upper Carnian or younger) is based on lithostratigraphic comparison to other dated sections (see below), introducing a significant margin of error for precise chronological considerations. Therefore, due to unresolved ambiguities in the interpretation of bone extensions in ML. A9182, and to a smaller extent in *H. chelyops*, we identify ML. A9182 as *Henodus* sp. and at this point refrain from taxonomic assignment at a species level. Thus, a better understanding of the variation within the German material of *H. chelyops* and/or new material from the Algarve are necessary for more conclusive interpretations.

Temporal Range of Henodontidae

Henodus chelyops was thought to be recovered from the Estherienschichten deposits (Reiff, 1937; von Huene, 1936), which constitute the uppermost part of the Lower Gipskeuper succession, also known as Grabfeld Formation (Aigner & Bachmann, 1989; Menning, 2018). The Grabfeld Fm. spans across Longobardian and Julian (late Middle Triassic and early Late Triassic), with its upper portion including the Estherienschichten, being interpreted as Julian in age, corresponding to lower Carnian (Menning, 2018; Zeh et al., 2021; Zhang et al., 2020). In some works, the upper portion of Grabfeld Fm. is assigned to Cordevolian (e.g., Bachmann & Kozur, 2004)—the term which is equivalent to early Julian sensu Ogg et al. (2020) or mid-late Julian sensu Zhang et al. (2020) and Zeh et al. (2021). However, as the site where *H. chelyops* had been found has been drastically changed (no more access to sedimentary rock exposure) the outlined stratigraphic interpretation cannot be entirely confirmed. Moreover, the *H. chelyops* remains were suggested to potentially derive from a younger unit, namely the Gaildorf-horizon of the Lower Schilfsandstein (Stuttgart Fm.), corresponding to middle Carnian (personal communication Günter Schweigert in 2023, see also Geyer et al., 2023). Nonetheless, until further detailed studies clarify the stratigraphic assignment of the *Henodus*-bearing levels, the historical classification within the Estherienschichten deposits should still be considered.

The palynological study of the El Atance deposits bearing *Parahenodus atancensis* indicates a (likely lowermost) Julian (García-Ávila et al., 2021), thus early Carnian age.

The base of the Silves Group in the Algarve region was established to correspond to lower to middle Carnian, being most likely lower Carnian in age (Vilas-Boas et al., 2022). Therefore, if armor plates from the São Bartolomeu de Messines are attributed to the locally occurring basal unit of Silves Group-São Bartolomeu de Messines Claystones–and are considered as belonging to *Henodus*, that would imply a roughly coeval occurrence of that genus in the Algarve together with *H. chelyops* from Germany. Nonetheless, as discussed above, taxonomic

assignation at lower taxonomic levels is very problematic in the case of isolated armor plates. Moreover, the attribution of São Bartolomeu de Messines outcrop to São Bartolomeu de Messines Claystones also remains uncertain (see Geological setting). Therefore, the occurrence of *Henodus* at the early to middle Carnian interval of the Algarve Basin remains contested.

The *Henodus* cranium recovered in the Algarve comes from a younger unit (Silves Marl-Carbonate Evaporitic Complex, sensu Vilas-Boas et al., 2024), which was constrained to be upper Carnian to Rhaetian/Hettangian in age. However, the site containing the described cranium lacks a precise age estimate. Despite attempts to palynologically date the site, samples obtained from Vale do Álamo and Rocha da Pena turned out to be palynologically sterile (Vilas-Boas personal communication). Thus, placodont remains including the *Henodus* cranium uncovered within the Marl-Carbonate Evaporitic Complex are of younger, but precisely unknown, age when compared with both *Parahenodus atancensis* and *Henodus chelyops* from the Grabfeld Fm., extending the temporal range of Henodontidae.

Paleobiogeography of Henodontidae

All henodontid placodont-bearing sites correspond to the low latitude situated areas during the Late Triassic (ca. 15–30°N), located at the Laurasian continental margin (Fig. 10) in proximity to the Neotethys Ocean (Golonka, 2007; van Hinsbergen et al., 2015; Scotese & Schettino, 2017).

The presented cranial, and the potential postcranial (i.e., dermal plates), material from the Algarve constitutes the second recorded occurrence of *Henodus*, which so far has been exclusively known from the Goldersbach near Tübingen-Lustnau situated in southwestern Germany, which represents the southern portion of the Germanic Basin (Aigner & Bachmann, 1989; Franz et al., 2015; von Huene, 1936). The Algarve record extends the paleogeographic range of that genus outside of the Germanic Basin and enlarges it to the Laurasian coastal area near the western-most branch of the Neotethys (for interpretation of paleogeographic setting see Arche & López-Gómez, 2014; Gama et al., 2021; Ortí et al., 2017; Pereira et al., 2017).

The fact that *Henodus* remains were found in those two distant areas demonstrates its distinct geographic distribution. Based on those occurrences, it seems possible that *Henodus* could have occupied either freshwater or brackish to shallow marine habitats (see below) within the south-western coast of Laurasia stretching along the occidental part of the Neotethys (Fig. 10).

The newly presented record of *Henodus* in the Algarve region contradicts the hypothesis of its endemic occurrence within the Germanic Basin. It was previously suggested that the apparent endemism of *Henodus* in the Germanic Basin might be a result of population isolation following the regressive phase during the Late Ladinian, leading to the retreat of epicontinental seas in continental Europe (Pinna, 1990). If applying Pinna's (1990) hypothesis to the novel Algarve record, the localized occurrence of isolated *Henodus* populations along parts of the occidental Neotethys/Laurasian coast during the early Late Triassic remains a possibility. However, this would imply an earlier occurrence and a relatively broad distribution of the genus before the regression event. Alternatively, considering a likely younger age of the Algarve record, upper Carnian or younger, dispersion events of *Henodus* at some point during the Late Triassic can also be considered. Nevertheless, the scarcity of the *Henodus* record hinders any further discussion on the paleobiogeographic history of this taxon.

The presented occurrence of *Henodus* is the second record of the Henodontidae in the Iberian Peninsula, after the discovery of the *P. atancensis* (de Miguel Chaves et al., 2018a, 2020c; García-Ávila et al., 2021). Despite occurring in separate basins and at distinct distances from each other, the novel *Henodus* material illustrates that both henodontid genera were present in the Iberia near the westernmost part of the Neotethys (Fig. 10).

Paleoecology of Henodontidae

The sedimentological record of the Upper Triassic Silves Marl-Carbonate Evaporitic Complex in the Algarve indicates environmental conditions characterized by the deposition of interlayered evaporite-rich mudstones and limestones (see Supplementary File 1) under semi-arid climates, in floodplain and palustrine environments (Ruciński, 2020). Due to the continental depositional setting prevalent in the studied area, the paleoenvironment inhabited by *Henodus* most likely represented either a freshwater/water body or a brackish water environment (Vilas-Boas et al., 2024). In the palynological study, Vilas-Boas et al. (2024) suggested coastal-lacustrine to sabkha environments for Silves Marl-Carbonate Evaporitic Complex, with an increased content of algal spores (i.e., *Plaesiodictyon mosellanum*, *Botryococucus* spp., *Ovoidities* sp.), implying likely brackish conditions. A continental but near coastal depositional setting with alternating shallow marine influence was also indicated by regional geological and geochemical studies of the Algarve Upper Triassic deposits (Azerêdo et al., 2003; Palain, 1976, 1979; Santos et al., 2022; Trindade et al., 2010). So far, all placodont remains at all recorded sites have been identified exclusively in carbonate or calcareous-rich beds, often associated with evaporites, which could suggest a potential linkage of their occurrence with water bodies characterized by fluctuating and likely overall elevated salinity.

Within the strata containing placodont fossils in the Algarve, no invertebrate material has been found so far, while discernible vertebrate remains are exclusively comprised of actinopterygian and chondrichthyan remains (Ruciński, 2020). This conspicuous absence of invertebrates may be attributable to sampling bias or, more likely, a taphonomic bias resulting from the depletion of invertebrate records due to the dissolution of aragonitic remains in beds highly affected by pedogenesis (Ruciński, 2020). Nevertheless, a Late Triassic bivalve and gastropod assemblage was retrieved from the easternmost sector of the Algarve Basin, in sections near the Ayamonte town (Santos et al., 2022). These sections are construed as a succession of continental (alluvial) to marginal and shallow marine deposits, marked by oscillating marine episodes and freshwater influence (Santos et al., 2022). This fauna manifests moderate taxonomic diversity and is notably characterized by the prevalently diminutive size of specimens, typically not exceeding a few millimeters in diameter (Santos et al., 2022). Additionally, a sauropterygian neural arch has been unearthed in the discussed deposits (Reolid et al., 2022; Santos et al., 2022).

The Grabfeld Fm. contains shales, nodular gypsum, salt, and pedogenic deposits formed in the succession of sabkha, coastal playa, and salina environments under the arid climate (Aigner & Bachmann, 1989; Franz et al., 2014; Shukla et al., 2010). According to Richter (1985) and Aigner and Bachmann (1989), some carbonates correspond to temporal marine ingressions, while the dolomites of the Estherienschichten, where *H. chelyops* was found, represent playa dolomites formed in the coastal salina mudflat setting. Consequently, they are likely associated with alternating freshwater to brackish and saline environments. Some interpretations characterize this setting as a restricted brackish lagoon exhibiting seasonal desiccation and significant salinity fluctuations (Mazin & Pinna, 1993; Pommery et al., 2021). Alternatively, if considering the proposed Schilfsandstein provenance of

the *Henodus* remains (Geyer et al., 2023), a lacustrine or lagoonal setting within an overall fluvio-deltaic system can be considered (Franz et al., 2014; Geyer et al., 2023; Shukla et al., 2010). The fauna retrieved from *Henodus*-bearing layers is notably sparse in terms of both abundance and diversity. It predominantly comprises estherid conchostracans, with rare occurrences of gastropods and actinopterygians (Pommery et al., 2021; Reif & Stein, 1999; Reiff, 1937; von Huene, 1936).

The Keuper siliciclastic to evaporitic facies in central Spain delineate coastal and shallow marine environments, transitioning spatially from alluvial plains and mudflats to coastal sabkha and shallow marine settings (García-Ávila et al., 2021). The El Atance site, bearing *P. atacensis* cranium, is attributed to the El Puente Formation. This formation is characterized by black lutite facies exhibiting sedimentological features indicative of predominantly low-energy conditions (García-Ávila et al., 2021). The depositional setting at El Atance is interpreted as a spatially extensive shallow water lagoon. The inference of brackish conditions is drawn from sedimentological features indicative of a restricted connection to the open sea, the prevalence of typically freshwater to brackish green algae such as *Plaesiodictyon mosellanum*, and the presence of sauropterygians, which are typically associated with marine environments (García-Ávila et al., 2021). In addition to *P. atacensis*, sauropterygians at this site include the simosaurid *Paludidraco multidentatus* de Miguel Chaves 2018 and indeterminate nothosaurs (de Miguel Chaves et al., 2018b; García-Ávila et al., 2021).

Considering the paleogeographic position and geological settings, it appears plausible that all known representatives of Henodontidae inhabited (near) coastal water bodies or shallow brackish lagoons within arid to semi-arid climates. Their habitat was quite likely subjected to high environmental fluctuation as suggested by mixed siliciclastic and carbonate, and overall evaporite rich, deposition with palynological data further indicating a complex interplay of marine and freshwater influences within the depositional settings. The observed low-diversity assemblages, characterized predominantly by small-sized fauna, may indicate environmental stress in the discussed habitats. However, uncertainties persist regarding the extent to which taphonomic processes may have influenced the observed low taxonomic diversity.

In summary, currently available records of Henodontidae point to the adaptation of these organisms to the colonization of habitats characterized by stringent environmental conditions within restricted marine, coastal brackish, and conceivably coastal freshwater settings. Some authors (Gere et al., 2024; Pinna, 1990; Rieppel, 2002a, 2002b) already hypothesized that development of unique morphological features such as enormous carapace and plastron (hypothesized to serve a function of an osmotic barrier), as well as cranial modifications (adaptation to either filter feeding, herbivory or more likely generalist diet), can be possibly linked to the adaptation of *Henodus* to environments with depleted larger hard-shelled prey and highly fluctuating environmental conditions. Those conditions were noted to be more prevalent in the wake of the end-Ladinian regression event in areas corresponding to modern western Europe and thus coinciding with the Carnian record of Henodontidae. Our new study cannot confirm the outlined assumptions but existing data on paleoecology and paleoenvironmental settings of henodontid placodonts, including the novel Algarve material, appear at this point to be concordant with the previously proposed hypothesis.

CONCLUSIONS

Paleontological fieldwork conducted in the Algarve (southern Portugal) have unveiled an assemblage of placodont material originating from four sites and spanning multiple stratigraphic levels. The amassed collection predominantly comprises dermal armor plates, which can be classified into two distinct morphotypes. Morphotype 1, characterized by elongated hexagonal plates, is identified as Cyamodontoidea cf. *Henodus*. Meanwhile, morphotype 2, featuring equilateral osteoderms, is assigned to Cyamodontoidea indet. Both morphotypes might refer to specimens derived from distinct portions of the *Henodus* carapace, however, due to poor preservation and lack of associated material, this assumption cannot be confirmed.

The most informative placodont element (ML. A9182) is identified as a portion of the *Henodus* cranium. Assignation to *Henodus* sp. is based on i.a. the rectangular shape of the skull, the presence of a spatulate rostrum with toothless maxillae exhibiting curved grooves, and the separation of palatines by the pterygoids. However, preservation and ambiguities in the interpretations of bones currently prevent taxonomic identification at the species level.

The ML. A9182 specimen constitutes the first discovery of *Henodus* since 1959 and the first record of that animal outside its type locality at the Goldersbach site near Tübingen–Lustnau in Germany. Thus, this new find extends the paleobiogeographic range of the previously supposed endemic *Henodus*, outside of the Germanic Basin, to the Laurasian coast of the westernmost branch of the occidental part of the Neotethys.

The chronostratigraphic constraints of the ML. A9182 bearing deposits are at this moment very poorly defined as likely relating to upper Carnian-Rhaetian range. This suggests a younger age compared with previous early Carnian records of *Henodus* and *Parahenodus* (or potentially the middle Carnian in the case of the former).

The discovery of the Algarve material assigned to *Henodus* in an area characterized by continental mixed siliciclastic-carbonate deposition, likely situated in the proximity of the Neotethys, concurs with earlier findings of *Henodus* and *Parahenodus* derived from coastal environments. The henodontid material collected thus far, coupled with its paleoenvironmental context, indicates that this group of derived cyamodontoid placodonts was adapted to brackish (and possibly freshwater) habitats characterized by likely medium to low faunal diversity.

ACKNOWLEDGMENTS

We would like to thank anonymous reviewers for providing a detailed and very constructive review, contributing to the enhancement of the manuscript. We express our great gratitude to J. Graça for donating the skull ML. A9182 to the Museu Municipal de Loulé, making this study possible. Without this donation our knowledge of placodont material from the Algarve would be much poorer. We want to thank Geoparque Algarvensis for the support and promotion of this work. We want to thank Dinopark Lourinhã for enabling access to Dinopark's preparatory lab, helping in the process of preparation of the fossil material. We thank S. Mateus, J. Marinheiro, and V. López Rojas for support during the preparation in Dinopark Lourinhã as well as Nathalie Rodrigues for assistance in the preparation of armor plate material at the Museum of Lourinhã. We would also like to thank C. Pessoa for helping with XRF analysis at the Departamento de Ciências da Terra of Faculdade de Ciências e Tecnologia of Universidade Nova de Lisboa. We are also grateful to J. Kowalski and P. Janecki for providing illustration of *Henodus*. IW was funded by Deutsche Forschungsgemeinschaft (grant: WE5440/6-1) as well as by E. and W. Datz-Stiftung.

AUTHOR CONTRIBUTIONS

HC, MR, OM participated in fieldwork in the Algarve region, which resulted in the collection of the described material. The

geological setting was described by MR and HC. MR and HC described and compared the gathered fossil material, with revisions by OM. IW facilitated specimen comparison. Phylogeny analysis was done by MR. Phylogenetic matrix revision was performed by MR and IW. XRF analysis was performed by MR. Taxonomic identification was discussed by all authors. Figures were prepared by MR and HC. 3D models were created by MR, HC, and OM. All authors edited the manuscript. The paper is based on the initial results obtained for the thesis submitted by MR and HC for their MSc in Palaeontology at the Universidade Nova de Lisboa, which was supervised by OM. Work and analysis were continued and finalized after completion of MSc degrees by MR and HC at the University of Oslo and District Council of Loulé, respectively.

DATA AVAILABILITY STATEMENT

The data supporting and necessary to replicate the findings of the study are available within the paper and its Supplementary Information. The phylogeny data matrix, characters list and images are also available in Morphobank project 5220 at http://morphobank.org/permalink/?P5625.

DISCLOSURE STATEMENT

No potential conflict of interest was reported by the author(s).

ORCID

Maciej Ruciński http://orcid.org/0000-0003-0431-2960
Octávio Mateus http://orcid.org/0000-0003-1253-3616
Ingmar Werneburg http://orcid.org/0000-0003-1359-2036

SUPPLEMENTARY FILES

Supplementary File 1: Supplementary descriptions and figures presenting: geographic and stratigraphic contexts of ML. A9182; additional documentation of ML. A9182; preliminary stratigraphic context of other placodont remains in the studied sections in the central Algarve; details of phylogenetic analysis and character list including indicated modifications of Neenean et al. (2015) data.

Supplementary File 2: XRF data used for stratigraphic considerations of block containing ML. A9182 including raw data, processed data for multivariate analyses and PCA loadings.

Supplementary File 3: Phylogenetic matrix (used for Analysis 1) based on the comprehensive diapsid matrix of Wang et al. (2022).

Supplementary File 4: Phylogenetic matrix (used for Analysis 2) based on the comprehensive diapsid matrix of Neenan et al. (2015) with incorporated modifications presented in Wang et al. (2019a).

Supplementary File 5: Phylogenetic cranial character matrix (used for Analysis 3) based on Neenan et al. (2015).

Supplementary File 6: Phylogenetic cranial character matrix (used for Analysis 4) with modified scoring based on Neenan et al. (2015).

Supplementary File 7: 3D model of ML. A9182.

LITERATURE CITED

Aigner, T., & Bachmann, G. H. (1989). Dynamic stratigraphy of an evaporite-to-red bed sequence, Gipskeuper (Triassic), southwest German Basin. *Sedimentary Geology*, *62*(1), 5–25. https://doi.org/10.1016/0037-0738(89)90098-5

Arche, A., & López-Gómez, J. (2014). The Carnian Pluvial Event in Western Europe: New data from Iberia and correlation with the Western Neotethys and Eastern North America–NW Africa regions. *Earth-Science Reviews*, *128*, 196–231. https://doi.org/10.1016/j.earscirev.2013.10.012

Azerêdo, A. C., Duarte, L. V., Henriques, M. H., & Manuppella, G. (2003). Da dinâmica continental no Triásico aos mares do Jurássico Inferior e Médio. *Cadernos de Geologia de Portugal*, Instituto Geológico Mineiro, Portugal, p. 43.

Bachmann, G. H., & Kozur, H. W. (2004). The Germanic Triassic: correlations with the international chronostratigraphic scale, numerical ages and Milankovitch cyclicity. *Hallesches Jahrbuch für Geowissenschaften*, *26*, 17–62.

Benton, M. J. (2014). *Vertebrate palaeontology*. John Wiley & Sons.

Benton, M. J., & Wu, F. (2022). Triassic Revolution. *Frontiers in Earth Science*, *10*, https://doi.org/10.3389/feart.2022.899541

Benton, M. J., Zhang, Q., Hu, S., Chen, Z.-Q., Wen, W., Liu, J., Huang, J., Zhou, C., Xie, T., Tong, J., & Choo, B. (2013). Exceptional vertebrate biotas from the Triassic of China, and the expansion of marine ecosystems after the Permo-Triassic mass extinction. *Earth-Science Reviews*, *125*, 199–243. https://doi.org/10.1016/j.earscirev.2013.05.014

Brusatte, S. L., Butler, R. J., Mateus, O., & Steyer, J. S. (2015). A new species of *Metoposaurus* from the Late Triassic of Portugal and comments on the systematics and biogeography of metoposaurid temnospondyls. *Journal of Vertebrate Paleontology*, *35*(3), e912988. https://doi.org/10.1080/02724634.2014.912988

Buffetaut, E., & Novak, M. (2008). A cyamodontid placodont (Reptilia: Sauropterygia) from the Triassic of Slovenia. *Palaeontology*, *51*(6), 1301–1306. https://onlinelibrary.wiley.com/doi/10.1111/j.1475-4983.2008.00819.x https://doi.org/10.1111/j.1475-4983.2008.00819.x

Campos, H., & Mateus, O. (2018). *The first record of placodonts in Portugal and its chronological and paleoecological implications. [Poster presentation]*. XVI annual meeting of the European Association of Vertebrate Palaeontologists, Caparica, Portugal.

Campos, H., Mateus, O., & Moreno-Azanza, M. (2017). Preliminary results on the stratigraphy and taphonomy of multiple bonebeds in the Triassic of Algarve. *XV Encuentro de Jóvenes Investigadores en Paleontología, Pombal, Portugal*, 83–87.

Cheng, L., C. Moon, B., Yan, C., Motani, R., Jiang, D., An, Z., & Fang, Z. (2022). The oldest record of Saurosphargiformes (Diapsida) from South China could fill an ecological gap in the Early Triassic biotic recovery. *PeerJ*, *10*, e13569. https://doi.org/10.7717/peerj.13569

Choffat, P. (1887). Recherches sur les terrains secondaires au Sud du Sado. *Commissão dos Trabalhos Geológicos de Portugal*, *1*, 222–312.

Choffat, P. (1904). L'Infralias et le Sinémurien du Portugal. *Comunicações Dos Serviços Geológicos de Portugal*, *5*, 49–117.

Chun, L., Rieppel, O., Long, C., & Fraser, N. C. (2016). The earliest herbivorous marine reptile and its remarkable jaw apparatus. *Science Advances*, *2*(5), e1501659. DOI: 10.1126/sciadv.1501659

Clark, W. (1976). The environment and the genotype in polymorphism. *Zoological journal of the Linnean Society*, *58*(3), 255–262. https://doi.org/10.1111/j.1096-3642.1976.tb00831.x

Cope, E. (1871). The systematic arrangement of the Reptilia. *Proceedings of the American Association for the Advancement of Science*, *19*, 226–247.

Dalrymple, G. H. (1977). Intraspecific Variation in the Cranial Feeding Mechanism of Turtles of the Genus *Trionyx* (Reptilia, Testudines, Trionychidae). *Journal of herpetology*, *11*(3), 255–285. https://doi.org/10.2307/1563241

de la Fuente, M. S., Sterli, J., & Krapovickas, V. (2021). Triassic turtles from Pangea: The legacy from South America. *Journal of South American Earth Sciences*, *105*, 102910. https://doi.org/10.1016/j.jsames.2020.102910

de Miguel Chaves, C., Ortega, F., & Pérez-García, A. (2018b). New highly pachyostotic nothosauroid interpreted as a filter-feeding Triassic marine reptile. *Biology Letters*, *14*(8), 20180130. https://doi.org/10.1098/rsbl.2018.0130

de Miguel Chaves, C., Ortega, F., & Pérez-García, A. (2020b). The Iberian Triassic fossil record of Sauropterygia: an update. *Journal of Iberian Geology*, *46*(4), 445–464. https://doi.org/10.1007/s41513-020-00137-w

de Miguel Chaves, C., Ortega, F., & Pérez-García, A. (2018a). A new placodont from the Upper Triassic of Spain provides new insights on the acquisition of the specialized skull of Henodontidae. *Papers in Palaeontology*, *4*(4), 567–576. https://doi.org/10.1002/spp2.1218

de Miguel Chaves, C., Pérez-García, A., Cobos, A., Royo-Torres, R., Ortega, F., & Alcala, L. (2015). A diverse Late Triassic tetrapod fauna from Manzanera (Teruel, Spain). *Geobios*, *48*(6), 479–490. https://doi.org/10.1016/j.geobios.2015.09.002

de Miguel Chaves, C., Scheyer, T. M., Ortega, F., & Pérez-García, A. (2020a). The placodonts (Sauropterygia) from the Middle Triassic of Canales de Molina (Central Spain), and an update on the knowledge about this clade in the Iberian record. *Historical Biology*, *32*(1), 34–48. https://doi.org/10.1080/08912963.2018.1462805

de Miguel Chaves, C., Serrano, A., Ortega, F., & Perez-Garcia, A. (2020c). Braincase and endocranium of the placodont *Parahenodus atancensis* de Miguel Chaves, Ortega & Pérez-García, 2018, a representative of the highly specialized clade Henodontidae. *Comptes Rendus Palevol*, *19*(10), 173–186.

Fischer, W. (1959). Neue Funde von *Henodus chelyops* v. Huene im Tübinger Gipskeuper. *Neues Jahrbuch für. Geologie und Paläontologie*, *6*, 241–247.

Foth, C., Bona, P., & Desojo, J. B. (2015). Intraspecific variation in the skull morphology of the black caiman *Melanosuchus niger* (Alligatoridae, Caimaninae). *Acta Zoologica*, *96*(1), 1–13. https://doi.org/10.1111/azo.12045

Franz, M., Kaiser, S. I., Fischer, J., Heunisch, C., Kustatscher, E., Luppold, F. W., Berner, U., & Röhling, H. G. (2015). Eustatic and climatic control on the Upper Muschelkalk Sea (late Anisian/Ladinian) in the Central European Basin. *Global and Planetary Change*, *135*, 1–27. https://doi.org/10.1016/j.gloplacha.2015.09.014

Franz, M., Nowak, K., Berner, U., Heunisch, C., Bandel, K., Röhling, H. G., & Wolfgramm, M. (2014). Eustatic control on epicontinental basins: The example of the Stuttgart Formation in the Central European Basin (Middle Keuper, Late Triassic). *Global and Planetary Change*, *122*, 305–329. https://doi.org/10.1016/j.gloplacha.2014.07.010

Gaffney, E. S. (1990). The comparative osteology of the Triassic turtle *Proganochelys*. *Bulletin of the American Museum of Natural History*, *194*, 259p.

Gama, C., Pereira, M. F., Crowley, Q. G., Dias da Silva, Í, & Silva, J. B. (2021). Detrital zircon provenance of Triassic sandstone of the Algarve Basin (SW Iberia): evidence of Gondwanan- and Laurussian-type sources of sediment. *Geological Magazine*, *158*(2), 311–329. https://doi.org/10.1017/S0016756820000370

García-Ávila, M., De la Horra, R., de Miguel Chaves, C., Juncal, M. A., Pérez-García, A., Ortega, F., & Diez, J. B. (2021). Palynological and sedimentological implications of the sauropterygian Upper Triassic site of El Atance (Central Iberian Peninsula). *Review of Palaeobotany and Palynology*, *295*, 104541. https://doi.org/10.1016/j.revpalbo.2021.104541

Gere, K., Nagy, A. L., Scheyer, T. M., Werneburg, I., & Ösi, A. (2024). Complex dental wear analysis reveals dietary shift in Triassic placodonts (Sauropsida, Sauropterygia). *Swiss Journal of Palaeontology*, *143*(1), 4. https://doi.org/10.1186/s13358-024-00304-x

Gere, K., Scheyer, T. M., Makádi, L., & Ösi, A. (2020). Placodont remains (Sauropsida, Sauropterygia) from the Triassic of Hungary (Transdanubian Range and Villány Mountains). *Palaeobiodiversity and Palaeoenvironments*, *100*(4), 1047–1063. https://doi.org/10.1007/s12549-020-00432-5

Geyer, M., Nitsch, E., & Simon, T. (2023). *Geologie von Baden-Württemberg (6. völlig neu bearbeitete Auflage)*.

Golonka, J. (2007). Late Triassic and Early Jurassic Palaeogeography of the world. *Palaeogeography, palaeoclimatology, palaeoecology*, *244*(1), 297–307. https://doi.org/10.1016/j.palaeo.2006.06.041

Haas, G. (1967). On the vertebral centra of nothosaurs and placodonts from the Muschelkalk of Wadi Ramon, Israel. *Coll int CNRS*, *163*, 329–334.

Haas, G. (1969). The armour of placodonts from the Muschelkalk of Wadi Ramon (Israel). *Israel journal of Zoology*, *18*(2–3), 135–147.

Jiang, D.-Y., Motani, R., Hao, W.-C., Rieppel, O., Sun, Y.-L., Schmitz, L., & Sun, Z.-Y. (2008). First record of placodontoidea (Reptilia, Sauropterygia, Placodontia) from the eastern Tethys. *Journal of Vertebrate Paleontology*, *28*(3), 904–908. https://www.jstor.org/stable/20491013 https://doi.org/10.1671/0272-4634(2008)28[904:FROPRS]2.0.CO;2

Klein, N., & Scheyer, T. M. (2013). A new placodont sauropterygian from the Middle Triassic of the Netherlands. *Acta Palaeontologica Polonica*, *59*(4), 887–902. https://doi.org/10.4202/app.2012.0147

Li, C., Jiang, D.-Y., Cheng, L., Wu, X.-C., & Rieppel, O. (2014). A new species of *Largocephalosaurus* (Diapsida: Saurosphargidae), with implications for the morphological diversity and phylogeny of the group. *Geological Magazine*, *151*(1), 100–120. doi:10.1017/S001675681300023X

Li, C., & Rieppel, O. (2002). A new cyamodontoid placodont from Triassic of Guizhou, China. *Chinese Science Bulletin*, *47*(5), 403–407. https://doi.org/10.1360/02tb9094

Li, C., Rieppel, O., Wu, X.-C., Zhao, L.-J., & Wang, L.-T. (2011). A New Triassic Marine Reptile from Southwestern China. *Journal of Vertebrate Paleontology*, *31*(2), 303–312. doi:10.1080/02724634.2011.550368

Lopes, F. (2014). Novas interpretações do Triásico da parte central da Bacia do Algarve (Portugal). *Comunicações Geológicas*, *101*.

Lyson, T. R., Rubidge, B. S., Scheyer, T. M., de Queiroz, K., Schachner, E. R., Smith, R. M., Botha-Brink, J., & Bever, G. (2016). Fossorial origin of the turtle shell. *Current Biology*, *26*(14), 1887–1894. https://doi.org/10.1016/j.cub.2016.05.020

Maddison, W. P., & Maddison, D. R. (2011). Mesquite: a modular system for evolutionary analysis. Version 3.81. Available at: http://mesquiteproject.org.

Maisch, M. W. (2020). The evolution of the temporal region of placodonts (Diapsida: Placodontia)–a problematic issue of cranial osteology in fossil marine reptiles. *Palaeodiversity*, *13*(1), 57. https://doi.org/10.18476/pale.v13.a6

Manuppella, G. (1992). *Carta Geológica da Região do Algarve.* [2 sheets at the 1:100.000 scale and Explanatory Note.]. Serviços Geológicos de Portugal.

Martin, J. E., Delfino, M., Garcia, G., Godefroit, P., Berton, S., & Valentin, X. (2016). New specimens of *Allodaposuchus precedens* from France: intraspecific variability and the diversity of European Late Cretaceous eusuchians. *Zoological Journal of the Linnean Society*, *176*(3), 607–631. https://doi.org/10.1111/zoj.12331

Martins, L. T., Madeira, J., Youbi, N., Munhá, J., Mata, J., & Kerrich, R. (2008). Rift-related magmatism of the Central Atlantic magmatic province in Algarve, Southern Portugal. *Lithos*, *101*(1), 102–124. https://doi.org/10.1016/j.lithos.2007.07.010

Mateus, O., Butler, R. J., Brusatte, S. L., Whiteside, J. H., & Steyer, J. S. (2014). The first phytosaur (Diapsida, Archosauriformes) from the Late Triassic of the Iberian Peninsula. *Journal of Vertebrate Paleontology*, *34*(4), 970–975. https://doi.org/10.1080/02724634.2014.840310

Mazin, J. M., & Pinna, G. (1993). Palaeoecology of the armoured placodonts. *Paleontologia Lombarda della Società Italiana di Scienze Naturali e del Museo Civico di Storia Naturale di Milano, Nuova serie*, *2*, 83–91.

Menning, M. (2018). Die Stratigraphische Tabelle von Deutschland 2016 (STD 2016). The Stratigraphic Table of Germany 2016 (STG 2016). *Zeitschrift der Deutschen Gesellschaft für Geowissenschaften*, *169*(2), 105–128. doi:10.1127/zdgg/2018/0161

Motani, R. (2009). The Evolution of Marine Reptiles. *Evolution: Education and Outreach*, *2*(2), 224–235. https://doi.org/10.1007/s12052-009-0139-y

Neenan, J. M., Klein, N., & Scheyer, T. M. (2013). European origin of placodont marine reptiles and the evolution of crushing dentition in Placodontia. *Nature Communications*, *4*(1), 1621. https://doi.org/10.1038/ncomms2633

Neenan, J. M., Li, C., Rieppel, O., & Scheyer, T. M. (2015). The cranial anatomy of Chinese placodonts and the phylogeny of Placodontia (Diapsida: Sauropterygia). *Zoological journal of the Linnean Society*, *175*(2), 415–428. https://doi.org/10.1111/zoj.12277

Neenan, J. M., & Scheyer, T. M. (2014). New specimen of *Psephoderma alpinum* (Sauropterygia, Placodontia) from the Late Triassic of Schesaplana Mountain, Graubünden, Switzerland. *Swiss Journal of Geosciences*, *107*(2–3), 349–357. https://doi.org/10.1007/s00015-014-0173-9

Nesbitt, S. J., Desojo, J. B., & Irmis, R. B. (2013). *Anatomy, phylogeny and palaeobiology of early archosaurs and their kin* (Vol. 379). The Geological Society of London London, Special Publication 379.

Norden, K. K., Duffin, C. J., & Benton, M. J. (2015). A marine vertebrate fauna from the Late Triassic of Somerset, and a review of British placodonts. *Proceedings of the Geologists' Association*, *126*(4–5), 564–581. https://doi.org/10.1016/j.pgeola.2015.07.001

Ogg, J., Chen, Z.-Q., Orchard, M., & Jiang, H. (2020). *The Triassic Period*. In *Geologic time scale 2020* (pp. 903–953). Elsevier.

Ortí, F., Pérez-López, A., & Salvany, J. M. (2017). Triassic evaporites of Iberia: Sedimentological and palaeogeographical implications for the western Neotethys evolution during the Middle Triassic–Earliest Jurassic. *Palaeogeography, Palaeoclimatology, Palaeoecology*, *471*, 157–180. https://doi.org/10.1016/j.palaeo.2017.01.025

Owen, R. (1860). *Palaeontology, or a systematic summary of extinct animals and their geological relations.* Adam and Charles Black.

Palain, C. (1976). Une série détritique terrigène les" Grès de Silves": Trias et Lias inférieur du Portugal. *Memória dos Serviços Geológicos de Portugal, Nova Série*, *25*, 377.

Palain, C. (1979). Connaissances stratigraphiques sur la base du Mésozoique portugais. *Ciências da Terra Univ Nova Lisboa*, *5*, 11–28.

Pereira, M. F., Ribeiro, C., Gama, C., Drost, K., Chichorro, M., Vilallonga, F., Hofmann, M., & Linnemann, U. (2017). Provenance of upper Triassic sandstone, southwest Iberia (Alentejo and Algarve basins): tracing variability in the sources. *International Journal of Earth Sciences*, *106*(1), 43–57. https://doi.org/10.1007/s00531-016-1295-2

Pérez-López, A., Cambeses, A., Pérez-Valera, F., & Götz, A. E. (2021). Rhaetian tectono-magmatic evolution of the Central Atlantic Magmatic Province volcanism in the Betic Cordillera, South Iberia. *Lithos*, *396–397*, 106230. https://doi.org/10.1016/j.lithos.2021.106230

Pinna, G. (1990). Notes on stratigraphy and geographical distribution of placodonts. *Atti della Società italiana di scienze naturali e del Museo civico di storia naturale di Milano*, *131*(7), 145–156.

Pinna, G., & Mazin, J. (1993). Stratigraphy and paleobiogeography of the Placodontia. *Paleontologia Lombarda Nuova Serie*, *2*, 125–130.

Pinna, G., & Nosotti, S. (1989). *Anatomia, morfologia funzionale e paleoecologia del rettile placodonte Psephoderma alpinum Meyer,* 1858. Memorie della Società ltaliana di Sci-enze Naturali e del Museo Civico di Storia Naturale di Milano 25, 17-50.

Pommery, Y., Scheyer, T. M., Neenan, J. M., Reich, T., Fernandez, V., Voeten, D. F., Losko, A. S., & Werneburg, I. (2021). Dentition and feeding in Placodontia: tooth replacement in *Henodus chelyops*. *BMC Ecology and Evolution*, *21*(1), 1–19. https://doi.org/10.1186/s12862-021-01835-4

Portela, P. R., Oliveira, R. J., Machado, F. P., Drehmer, C. J., Valente, A. L. S., & Dornelles, J. E. F. (2020). Morphology and intraspecific variation in the skull and mandible of the slider turtle *Trachemys dorbigni* (Testudines, Emydidae). *Zoomorphology*, *139*(3), 373–384. https://doi.org/10.1007/s00435-020-00491-4

Pratsch, J. C. (1958). Stratigraphisch-tektonische Untersuchungen im Mesozoikum von Algarve (Sudportugal). *Beihefte zum Geologischen Jahrbuch.*, *30*, 123.

Reif, W.-E., & Stein, F. (1999). Morphogeny and function of the dentition of *Henodus chelyops* Huene, 1936 (Placodontia, Triassic). *Neues Jahrbuch für Geologie und Paläontologie - Monatshefte*, 65–80.

Reiff, W. (1937). Ergebnisse der Grabung des Geologisch-Paläontologischen Universitäts-Instituts bei Tübingen-Lustnau im oberen Gipskeuper. *Zentralblatt für Mineralogie, Abteilung B*, *12*, 530–546.

Renesto, S., Dalla Vecchia, F.M. (2018). Late Triassic Marine Reptiles. In: Tanner, L. (eds) The Late Triassic World. Topics in Geobiology, vol 46. Springer, Cham. https://doi.org/10.1007/978-3-319-68009-5_8

Reolid, M., Muñiz Guinea, F., Toscano, A., & Belaústegui, Z. (2022). First record of fossil sauropterygians from the Upper Triassic of Southwestern Spain (Ayamonte, Huelva province). *Estudios Geológicos*, *78*(1), https://doi.org/10.3989/egeol.44639.613

Richter, D. K. (1985). Die Dolomite der Evaporit- und der Dolcrete-Playasequenz im mittleren Keuper bei Coburg (NE-Bayern). *Neues Jahrbuch für Geologie und Paläontologie - Abhandlungen*, *170*(1), 87–128. doi:10.1127/njgpa/170/1985/87

Rieppel, O. (2001). *The cranial anatomy of Placochelys placodonta Jaekel, 1902, and a review of the Cyamodontoidea (Reptilia, Placodonta) (Vol. Fieldiana, Geology, new series, no. 45)*. Field Museum of Natural History.

Rieppel, O. (2002a). Feeding mechanics in Triassic stem-group sauropterygians: the anatomy of a successful invasion of Mesozoic seas. *Zoological Journal of the Linnean Society*, *135*(1), 33–63. doi:10.1046/j.1096-3642.2002.00019.x

Rieppel, O. (2002b). The dermal armor of the cyamodontoid placodonts (Reptilia, Sauropterygia): morphology and systematic value. *Fieldiana: Geology*, *46*, 1–51.

Rieppel, O., Kuhn, O., Wellnhofer, P., & Appleby, R. M. (2000). *Sauropterygia I : Placodontia, Pachypleurosauria, Nothosauroidea, Pistosauroidea*. In P. Wellnhofer (Ed.), *Handbuch der Paläoherpetologie* (pp. 1–134). Verlag Friedrich Pfeil.

Rocha, R. B. (1976). Estudo estratigráfico e paleontológico do Jurássico do Algarve Ocidental. *Ciências da Terra, Universidade Nova de Lisboa*, *2*, 178.

Ruciński, M. R. (2020). *Novel placodont material and paleoenvironment analysis of Triassic deposits of Rocha da Pena (Algarve, southern Portugal)* [Master's thesis Universidade NOVA de Lisboa (Portugal)]. http://hdl.handle.net/10362/120738.

Russel, D., & Russel, D. (1977). Premiers résultats d'une prospection paléontologique dans le Trias de l'Algarve (Portugal). *Ciências da Terra/Earth Sciences Journal*, *3*.

Santos, A., Popovic, N., & Mayoral, E. (2022). Palaeoecology of Late Triassic marine assemblages from the proto-Atlantic Basin (Ayamonte, SW Spain). *Proceedings of the Geologists' Association*, *133*(1), 47–66. https://doi.org/10.1016/j.pgeola.2021.11.002

Scheyer, T. M. (2007). Skeletal histology of the dermal armor of Placodontia: the occurrence of 'postcranial fibro-cartilaginous bone' and its developmental implications. *Journal of Anatomy*, *211*(6), 737–753. https://doi.org/10.1111/j.1469-7580.2007.00815.x

Scheyer, T. M. (2010). New interpretation of the postcranial skeleton and overall body shape of the placodont *Cyamodus hildegardis* Peyer, 1931 (Reptilia, Sauropterygia). *Palaeontologia Electronica*, *13*(2), 15A.

Scheyer, T. M., & Klein, N. (2021). *Chapter 21: Sauropterygia: Placodontia*. In V. d. Buffrénil, A. d. Ricqlès, L. Zylberberg, K. Padian, M. Laurin, & A. Quilhac (Eds.), *Vertebrate Skeletal Histology and Paleohistology* (pp. 425–434). CRC Press.

Scheyer, T. M., Neenan, J. M., Bodogan, T., Furrer, H., Obrist, C., & Plamondon, M. (2017). A new, exceptionally preserved juvenile specimen of *Eusaurosphargis dalsassoi* (Diapsida) and implications for Mesozoic marine diapsid phylogeny. *Scientific Reports*, *7*(1), 4406. https://doi.org/10.1038/s41598-017-04514-x

Scheyer, T. M., Neenan, J. M., Renesto, S., Saller, F., Hagdorn, H., Furrer, H., Rieppel, O., & Tintori, A. (2011). Revised paleoecology of placodonts–with a comment on 'The shallow marine placodont *Cyamodus* of the central European Germanic Basin: its evolution, paleobiogeography and paleoecology'by CG Diedrich (Historical Biology, iFirst article, 2011, 1–19, doi: 10.1080/08912963.2011.575938). *Historical Biology*, *24*(3), 257–267. https://doi.org/10.1080/08912963.2011.621083

Scheyer, T. M., Oberli, U., Klein, N., & Furrer, H. (2022). A large osteoderm-bearing rib from the Upper Triassic Kössen Formation (Norian/Rhaetian) of eastern Switzerland. *Swiss Journal of Palaeontology*, *141*(1), 1. doi:10.1186/s13358-022-00244-4

Scheyer, T. M., Romano, C., Jenks, J., & Bucher, H. (2014). Early Triassic Marine Biotic Recovery: The Predators' Perspective. *PLoS One*, *9*(3), e88987. https://doi.org/10.1371/journal.pone.0088987

Schoch, R. R., & Sues, H. D. (2020). The origin of the turtle body plan: evidence from fossils and embryos. *Palaeontology*, *63*(3), 375–393. https://doi.org/10.1111/pala.12460

Scotese, C., & Schettino, A. (2017). Late Permian-Early Jurassic paleogeography of western Tethys and the world. In *Permo-Triassic salt provinces of Europe, North Africa and the Atlantic margins* (pp. 57–95). Elsevier. https://doi.org/10.1016/B978-0-12-809417-4.00004-5

Shukla, U. K., Bachmann, G. H., & Singh, I. B. (2010). Facies architecture of the Stuttgart Formation (Schilfsandstein, Upper Triassic), central Germany, and its comparison with modern Ganga system, India. *Palaeogeography, Palaeoclimatology, Palaeoecology*, *297*(1), 110–128. https://doi.org/10.1016/j.palaeo.2010.07.019

Soares, A. F., Kullberg, J. C., Marques, J. F., da Rocha, R. B., & Callapez, P. M. (2012). Tectono-sedimentary model for the evolution of the Silves Group (Triassic, Lusitanian basin, Portugal). *Bulletin de la Société géologique de France*, *183*(3), 203–216. https://doi.org/10.2113/gssgfbull.183.3.203

Stampfli, G. M., & Borel, G. D. (2002). A plate tectonic model for the Paleozoic and Mesozoic constrained by dynamic plate boundaries and restored synthetic oceanic isochrons. *Earth and Planetary Science Letters*, *196*(1), 17–33. https://doi.org/10.1016/S0012-821X(01)00588-X

Szczygielski, T., & Sulej, T. (2016). Revision of the Triassic European turtles *Proterochersis* and *Murrhardtia* (Reptilia, Testudinata, Proterochersidae), with the description of new taxa from Poland and Germany. *Zoological Journal of the Linnean Society*, *177*(2), 395–427. https://doi.org/10.1111/zoj.12374

Teixeria, C. (1942). Notas sôbre a Geologia do Triassico Português. *Boletim da Sociedade Geológica de Portugal*, *1*(3), 161–174.

Terrinha, P., Kullberg, J. C., Neres, M., Alves, T., Ramos, A., Ribeiro, C., Mata, J., Pinheiro, L., Afilhado, A., Matias, L., Luís, J., Muñoz, J. A.,

& Fernández, Ó. (2019). Rifting of the Southwest and West Iberia Continental Margins. In Quesada, C., Oliveira, J. (eds) The Geology of Iberia: A Geodynamic Approach. Regional Geology Reviews (pp. 251–283). Springer International Publishing. https://doi.org/10.1007/978-3-030-11295-0_6

Terrinha, P., Rocha, R., Rey, J., Cachão, M., Moura, D., Roque, C., Martins, L., Valadares, V., Cabral, J., & Azevedo, M. d. R. (2006). A Bacia do Algarve: Estratigrafia, paleogeografia e tectónica. *Geologia de Portugal no contexto da Ibéria*, 1–138.

Trindade, M. J., Rocha, F., & Dias, M. I. (2010). Geochemistry and mineralogy of clays from the Algarve Basin, Portugal: a multivariate approach to palaeoenvironmental investigations. *Current Analytical Chemistry*, *6*(1), 43–52.

van Hinsbergen, D. J. J., de Groot, L. V., van Schaik, S. J., Spakman, W., Bijl, P. K., Sluijs, A., Langereis, C. G., & Brinkhuis, H. (2015). A Paleolatitude Calculator for Paleoclimate Studies. *PLoS One*, *10*(6), e0126946. https://doi.org/10.1371/journal.pone.0126946

Verati, C., Rapaille, C., Féraud, G., Marzoli, A., Bertrand, H., & Youbi, N. (2007). $^{40}Ar/^{39}$ ages and duration of the Central Atlantic Magmatic Province volcanism in Morocco and Portugal and its relation to the Triassic–Jurassic boundary. *Palaeogeography, Palaeoclimatology, Palaeoecology*, *244*(1), 308–325. https://doi.org/10.1016/j.palaeo.2006.06.033

Vilas-Boas, M., Paterson, N. W., Pereira, Z., Fernandes, P., & Cirilli, S. (2022). The age of the first pulse of continental rifting associated with the breakup of Pangea in Southwest Iberia: new palynological evidence. *Journal of Iberian Geology*, *48*(2), 181–190. https://doi.org/10.1007/s41513-022-00189-0

Vilas Boas, M. (2023). *Palynology of the Triassic: Jurassic of the Silves Group in Portugal, its implications on a changing world*. [Doctoral dissertation, University of the Algarve] Dissertação de Doutoramento em Ciências do Mar, da Terra e do Ambiente, Ramo Geociências, Especialidade em Geologia, apresentada à Faculdade de Ciências e Tecnologia da Universidade do Algarve, 259 p. http://hdl.handle.net/10400.9/4300.

Vilas-Boas, M., Pereira, Z., Cirilli, S., Duarte, L. V., & Fernandes, P. (2021). New data on the palynology of the Triassic–Jurassic boundary of the Silves Group, Lusitanian Basin, Portugal. *Review of Palaeobotany and Palynology*, *290*, 104426. https://doi.org/10.1016/j.revpalbo.2021.104426

Vilas-Boas, M., Pereira, Z., Cirilli, S., & Fernandes, P. (2024). New Insights on the Upper Triassic Silves Group in Algarve Basin, Portugal: Palynological, paleophytogeography and paleoclimatology advances. *Geobios*, https://doi.org/10.1016/j.geobios.2024.08.001

von Huene, F. (1936). *Henodus chelyops*, ein neuer Placodontier. *Palaeontographica Abteilung A*, 99–147.

von Huene, F. (1938). Der dritte *Henodus*. Ergänzungen zur Kenntnis des Placodontiers *Henodus chelyops* Huene. *Palaeontographica Abteilung A*, 105–115.

von Huene, F. (1958). Nachträge zur Kenntnis von *Henodus chelyops* aus dem Tübinger Gipskeuper. *Palaeontographica Abteilung A*, 165–169.

von Nopcsa, F. (1923). Die Familien der Reptilien. *Fortschritte der Geologie und Paläontologie*, *2*, 1–210.

Wang, W., Li, C., Scheyer, T. M., & Zhao, L. (2019a). A new species of *Cyamodus* (Placodontia, Sauropterygia) from the early Late Triassic of south-west China. *Journal of Systematic Palaeontology*, *17*(17), 1457–1476. https://doi.org/10.1080/14772019.2018.1535455

Wang, W., Li, C., & Wu, X.-C. (2019b). An adult specimen of *Sinocyamodus xinpuensis* (Sauropterygia: Placodontia) from Guanling, Guizhou, China. *Zoological Journal of the Linnean Society*, *185*(3), 910–924. https://doi.org/10.1093/zoolinnean/zly080

Wang, W., Ma, F., & Li, C. (2020). First subadult specimen of *Psephochelys polyosteoderma* (Sauropterygia, Placodontia) implies turtle-like fusion pattern of the carapace. *Papers in Palaeontology*, *6*(2), 251–264. https://doi.org/10.1002/spp2.1293

Wang, W., Shang, Q., Cheng, L., Wu, X.-C., & Li, C. (2022). Ancestral body plan and adaptive radiation of sauropterygian marine reptiles. *iScience*, *25*(12), https://doi.org/10.1016/j.isci.2022.105635

Werneburg, I. (2021). 1934 bis 1957: *Henodus*: eine Tübinger Weltsensation. In E. Seidl, E. Bierende, & I. Werneburg (Eds.), *Aus der Tiefenzeit-Die Paläontologische Sammlung der Eberhard Karls Universität Tübingen* (pp. 442–451). Publikationen des Museums der Universität Tübingen (MUT).

Werneburg, I., & Böhme, M. (2018). The Palaeontologial Collection of Tübingen. In: *Paleontological Collections of Germany, Austria and Switzerland: The History of Life of Fossil Organisms at Museums and Universities*, 505–512. https://doi.org/10.1007/978-3-319-77401-5_52

Westphal, F. (1976). The dermal armour of some Triassic placodont reptiles. In A. D. A. Bellairs & C. B. Cox (Eds.), *Morphology and Biology of Reptiles* (pp. 31–41). London: Academic Press.

Wiens, J. J. (1999). Polymorphism in systematics and comparative biology. *Annual Review of Ecology and Systematics*, *30*(1), 327–362. https://doi.org/10.1146/annurev.ecolsys.30.1.327

Witzmann, F., & Gassner, T. (2008). Metoposaurid and mastodonsaurid stereospondyls from the Triassic–Jurassic boundary of Portugal. *Alcheringa: An Australasian Journal of Palaeontology*, *32*(1), 37–51. https://doi.org/10.1080/03115510701757316

Wolniewicz, A. S., Shen, Y., Li, Q., Sun, Y., Qiao, Y., Chen, Y., Hu, Y.-W., & Liu, J. (2023). An armoured marine reptile from the Early Triassic of South China and its phylogenetic and evolutionary implications. *eLife*, *12*, e83163. https://doi.org/10.7554/eLife.83163

Youbi, N., Martins, L. T., Munhá, J. M., Ibouh, H., Madeira, J., Aït Chayeb, E. H., & El Boukhari, A. (2003). *The Late Triassic-Early Jurassic Volcanism of Morocco and Portugal in the Framework of the Central Atlantic Magmatic Province: An Overview*. Washington, D. C: American Geophysical Union. https://doi.org/10.1029/136GM010

Zeh, A., Franz, M., & Obst, K. (2021). Zircon of Triassic Age in the Stuttgart Formation (Schilfsandstein)-Witness of Tephra Fallout in the Central European Basin and New Constraints on the Mid-Carnian Episode. *Frontiers in Earth Science*, *9*, https://doi.org/10.3389/feart.2021.778820

Zhang, Y., Ogg, J. G., Franz, M., Bachmann, G. H., Szurlies, M., Röhling, H.-G., Li, M., Rolf, C., & Obst, K. (2020). Carnian (Late Triassic) magnetostratigraphy from the Germanic Basin allowing global correlation of the Mid-Carnian Episode. *Earth and Planetary Science Letters*, *541*, 116275. https://doi.org/10.1016/j.epsl.2020.116275

Zhao, L.-J., Li, C., Liu, J., He, T., & Palasiatica, V. (2008). A new armored placodont from the Middle Triassic of Yunnan province, southwestern China. *Vertebrata Palasiatica*, *46*, 171–177.

Handling Editor: Hans-Dieter Sues.
Phylogenetics Editor: Pedro Godoy.